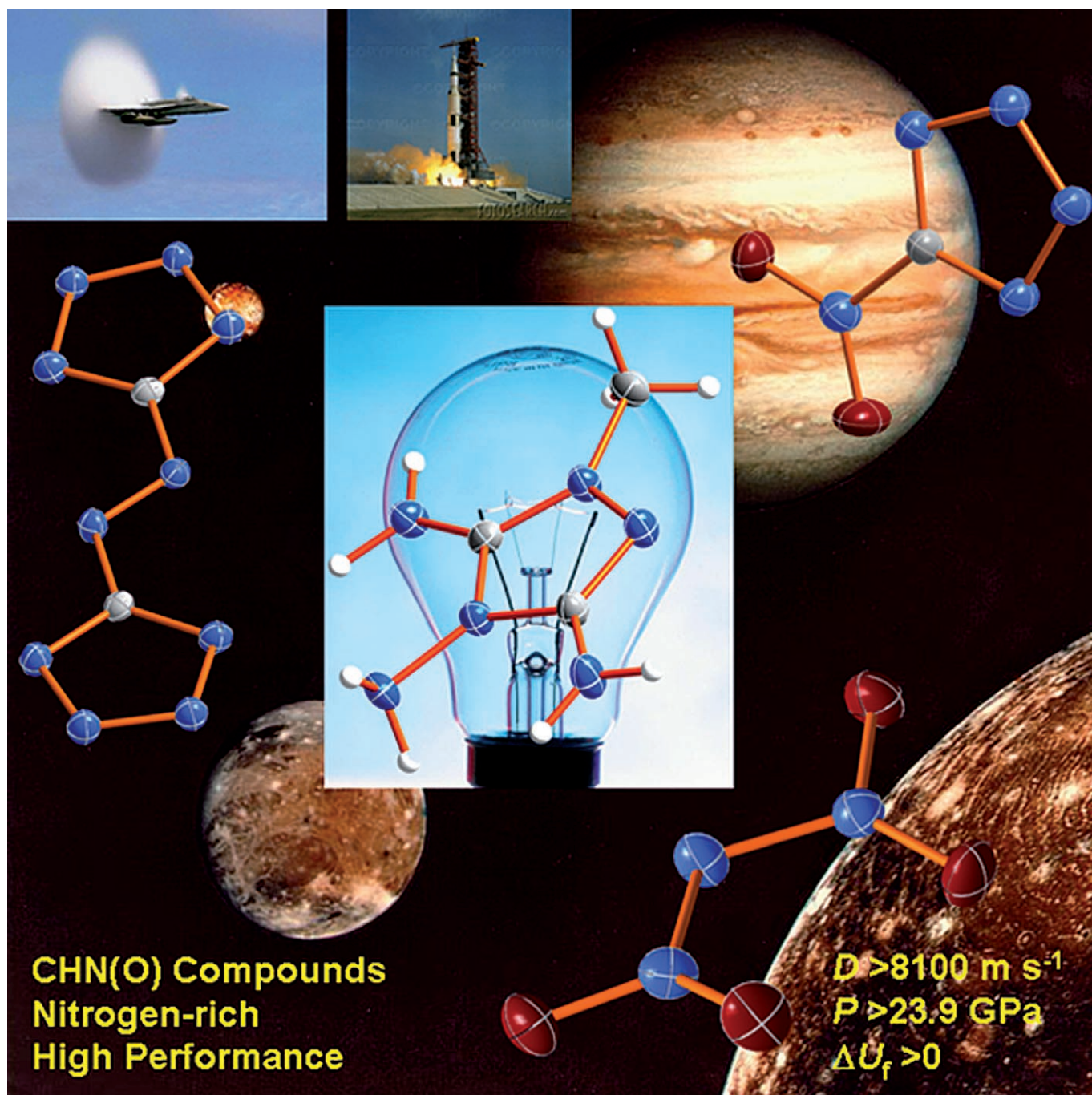


1,2,4-Triazolium-Cation-Based Energetic Salts

Chaza Darwich, Thomas M. Klapötke,* and Carles Miró Sabaté^[a]



Abstract: 3,4,5-Triamino-1,2,4-triazole (guanazine, **1**) can be readily methylated with methyl iodide yielding methylguanazinium iodide (**2**). Salts containing the novel methylguanazinium cation with energetic anions were synthesised by metathesis reactions with silver azide (**3**), silver nitrate (**4**), silver perchlorate (**5**), sodium 5,5'-azotetrazolate (**6**), silver 5-nitrotetrazolate (**7**) and silver dinitramide (**8**), yielding a new family of heterocycle-based salts, which were fully characterised by analytical (mass spectrometry and elemental analysis) and spectroscopic methods (IR, Raman and NMR). In addition, the molecular structures of all compounds were confirmed by X-ray anal-

ysis, revealing extensive hydrogen-bonding in the solid state and densities between 1.399 (**3**) and 1.669 g cm⁻³ (**5**). The hydrogen-bonded ring motifs are discussed in the formalism of graph-set analysis for hydrogen-bond patterns and compared to each other. Preliminary sensitivity testing of the crystalline compounds indicate surprisingly low sensitivities to both friction and impact, the highest friction and shock sensitivity being found for the perchlo-

Keywords: density functional calculations • energetic salts • graph-set analysis • nitrogen heterocycles • NMR spectroscopy

rate (**5**, 220 N) and the dinitramide (**8**, 20 J) salts, respectively. In addition, DSC analysis was used to assess the thermal stabilities of the compounds: **3–6** melt above 200 °C with concomitant decomposition, whereas **7** and **8** have clearly defined melting points at 162 and 129 °C, respectively, and with decomposition occurring about 30 °C above the melting point. Lastly all compounds have positive calculated heats of formation between 336 (**4**) and 4070 kJ kg⁻¹ (**6**) and calculated detonation velocities in the range between 8330 (**7**) and 8922 ms⁻¹ (**6**) making them of interest as new highly energetic materials with low sensitivity.

Introduction

The synthesis, characterisation and study of energetic materials have been the focus of our investigations over the last several years.^[1–7] There are several criteria that new high-energy density materials (HEDMs) should meet^[8] in order to be considered as feasible replacements for currently known energetic compounds, such as hexahydro-1,3,5-trinitro-1,3,5-triazine (RDX), trinitrotoluene (TNT) or pentaerythritol tetranitrate (PETN). Ideally, new compounds should have detonation parameters (e.g., velocity) comparable to those of known widely used high explosives (e.g., $D_{\text{RDX}} \approx 8800 \text{ ms}^{-1}$),^[9] good thermal stabilities of at least 200 °C, they should be hydrolytically stable with shelf lives longer than 15 years, be compatible with binders and/or plasticisers, insensitive to friction (>7 J) and shock (>120 N), have low (no) solubility in water, the decomposition products should be environmentally benign and the yield for their synthesis should be high and the price low. The performance of an energetic material is mainly a function of the density of the compound, its oxygen coefficient and its heat of formation; all three parameters are governed by its molecular structure.^[10] The higher the nitrogen content, the higher the heat of formation,^[11] which is in turn directly related to the performance of the material.

We are interested in azole-based energetic compounds with respect to the continuous interest in high-nitrogen ma-

terials as ingredients for propellants and explosives^[12,13] and are seeking for new energetic compounds with high densities and high positive heats of formation.^[14–16] Tetrazole-based energetic materials seem to show the best compromise between high heats of formation and good thermal stabilities. On the other hand, the presence of one carbon atom in the ring limits the introduction of functionality, whereas triazole-based energetic materials can be much more readily derivatised, for example, to the dinitro^[17] diamino^[18] or diazido^[19] compounds; the presence of two carbon atoms allows the easy introduction and/or combination of two of the aforementioned highly endothermic functional groups, allowing the formation of compounds with high positive heats of formation (i.e., high performances). Among others, triazolium-based energetic materials have found use as high explosives,^[20] gas generators^[21] and ionic liquids.^[22] This last material may possibly find application in melt-cast explosives.

Child et al.^[23a] were the first to synthesise 3,4,5-triamino-1,2,4-triazole (guanazine, **1**) by heating dimethylcyanamide with hydrazine hydrate under reflux. Recently, we discovered the potential of **1**, which has a nitrogen content of $\approx 73.6\%$, for the formation of nitrogen-rich energetic salts with anions such as 5-nitrotetrazolate,^[23b] picrate and 5,5'-azotetrazolate.^[24] Protonation of the triazole ring, proceeded unambiguously on N2/N3 from the triazole ring, rather than on the N–NH₂ or one of the C–NH₂ groups, as verified by X-ray diffraction studies. These are new examples of guanazinium salts, in addition to the already reported dinitramide, perchlorate and nitrate salts.^[25] However, an interesting azide salt has not been reported so far. Our experience in the laboratory indicates that due to the higher acidity of the guanazinium cation in respect to hydrazoic acid, guanazinium azide dissociates readily in solution to guanazine and hydrazoic acid. With this in mind, we synthesised guanazine

[a] Dr. C. Darwich, Prof. Dr. T. M. Klapötke, C. M. Sabaté
Department of Chemistry and Biochemistry
Energetic Materials Research, Ludwig-Maximilian University
Butenandstr. 5–13, 81377, Munich (Germany)
Fax: (+49) 89-2180-77492
E-mail: tmk@cup.uni-muenchen.de

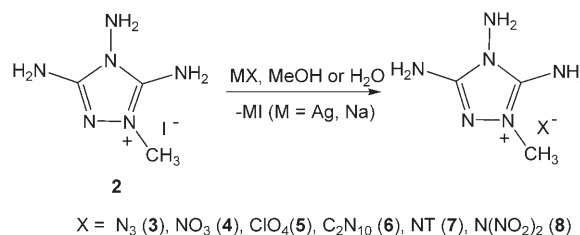
Supporting information for this article is available on the WWW under <http://www.chemeurj.org/> or from the author.

(1)^[23] and quaternised it with methyl iodide forming 1-methyl-3,4,5-triamino-1,2,4-triazolium iodide (MeGI, **2**), which had not been described in the literature prior to our studies,^[26] and surprisingly, had not been considered for the synthesis of energetic salts. We report here on the use of **2** as a useful starting material for the synthesis of energetic salts. The presence of the methyl group instead of a proton should not only allow us to obtain the highly endothermic azide compound, but also increase the thermal stability of the new materials, at the same time having reasonably high nitrogen contents, necessary for high heats of formations and environmentally friendly decomposition products. The presence of the three amino groups should lead to the formation of significantly hydrogen-bonded networks, which should result in high densities. Therefore, we decided to screen salt-based derivatives of methylguanazine with oxidising anions such as nitrate (**4**), perchlorate (**5**) and dinitramide (**8**), as well as with nitrogen-rich anions such as azide (**3**), 5,5'-azotetrazolate (**6**) and 5-nitrotetrazolate (**7**). The combination of the MeG⁺ ion with the above-mentioned oxidising anions yields **4**, **5** and **8**, which have better oxygen balances (Ω) values, that is, between -44 (dinitramide) and

-63% (nitrate), than, for example, TNT ($\Omega = -74\%$). The use of azide or azotetrazolate as the counteranion should give compounds with high positive heats of formation due to the nitrogen catenation, whereas the nitrotetrazolate salt should not only introduce endothermicity, but also improve the oxygen balance ($\Omega = -69\%$). However, the prediction of the crystal packing is often troublesome due to the multiplicity of structural possibilities and the lack of directionality of the intermolecular interactions. In consequence, it is important to closely examine the structural details, which may account for packing effects and, in last instance, for the properties of the compounds.

Results and Discussion

Synthesis: The synthesis of salts containing the methylguanazinium cation (**3–8**) was accomplished by metathesis of methylguanazinium iodide (**2**), prepared according to a previously reported procedure in our group,^[26] with one equivalent of a suitable energetic anion-transfer reagent (generally a silver salt). In the case of compound **6** the 5,5'-azotetrazolate transfer reagent used was the sodium salt (Scheme 1). In addition, the dinitramide salt **7** was alternatively and more safely prepared by reaction with silver(bispyridine) dinitramide [Ag(py)₂(N₃O₄)].^[27]



Scheme 1. Synthesis of methylguanazinium energetic salts **3–8** from iodide **2** (compounds **6** and **7** are monohydrate salts).

Quaternisation of the triazole ring by reaction of guanazine with methyl iodide to form the methylguanazinium cation, allowed us to prepare the azide salt (**3**), which could not be prepared with the guanazinium cation, due to the fact that protonated guanazine (GH⁺) protonates the azide anion to form guanazine and hydrazoic acid ($pK_a(\text{HN}_3) = 4.7$).^[30] This is in analogy to previous studies in our group on tetrazolium salts.^[31]

Vibrational and NMR spectroscopy: The most intense band in the Raman spectra (Figure 1) of the methylguanazinium salts synthesised corresponds to the vibration modes of the anions. They are observed at the following wavenumbers: 1347 cm⁻¹ (azide, $\nu(\text{N}_3)$),^[32] 1049 cm⁻¹ (nitrate, $\nu(\text{NO}_3)$),^[33] 936 and 462 cm⁻¹ (perchlorate, $\nu(\text{ClO}_4)$ and $\delta(\text{ClO}_4)$),^[34] 1373, 1410 and 1488 cm⁻¹ (azotetrazolate, $\nu_{\text{sym}}(\text{C}-\text{N}_{\text{azo}})$, $\nu_{\text{as}}(\text{C}-\text{N}_3)$ and $\nu(\text{N}_{\text{azo}}=\text{N}_{\text{azo}})$),^[13a] 1069 and 1418 cm⁻¹ (nitrotetrazolate, $\nu(\text{N}-\text{N}-\text{C})_{\text{ring}}$ and $\nu(\text{NO}_2)$)^[7b] and 1312 cm⁻¹ (dini-

Abstract in Spanish: 3,4,5-Triamino-1,2,4-triazol (guanazina, **1**) puede metilarse fácilmente con yodometano para formar yoduro de metilguanazino (**2**). Sales compuestas por el nuevo cation de metilguanazino con aniones energéticos fueron sintetizadas por metátesis del compuesto **2** con azida de plata (**3**), nitrato de plata (**4**), perchlorato de plata (**5**), 5,5'-azotetrazolato de sodio (**6**), 5-nitrotetrazolato de plata (**7**) y dinitramida de plata (**8**) dando lugar a la formación de una nueva familia de sales heterocíclicas. Los compuestos fueron caracterizados por métodos analíticos (espectrometría de masas y análisis elemental) y métodos espectroscópicos (IR, Raman y RMN). Además, la estructura molecular de los compuestos fué determinada por análisis de rayos X, revelando complejas redes unidas por enlaces de hidrogeno y densidades entre 1.399 (**3**) y 1.669 gcm⁻³ (**5**). Las redes formadas por los enlaces de hidrogeno se describen teniendo en cuenta un formalismo gráfico y se comparan entre ellas. Resultados preliminares acerca de la sensibilidad de los compuestos cristalinos muestran sales con sorprendente estabilidad. Los valores más bajos son alcanzados por las sales con el anion perchlorato (**5**, 220 N) y dinitramida (**8**, 20 J). Analisis calorimétricos (DSC) fueron usados para determinar la estabilidad térmica de los compuestos: **3–6** tienen puntos de fusión por encima de los 200°C con descomposición inmediata, mientras que **7** y **8** tienen puntos de fusión bien definidos a 162 y 129°C, respectivamente y temperaturas de descomposición alrededor de 30°C por encima. Todos las sales tienen energias de formación calculadas que toman valores positivos entre 336 (**4**) y 4070 kJkg⁻¹ (**6**) y velocidades de detonación calculadas entre 8330 (**7**) y 8922 ms⁻¹ (**6**) lo que los hace interesantes para el uso como nuevos compuestos altamente energéticos con baja sensibilidad.

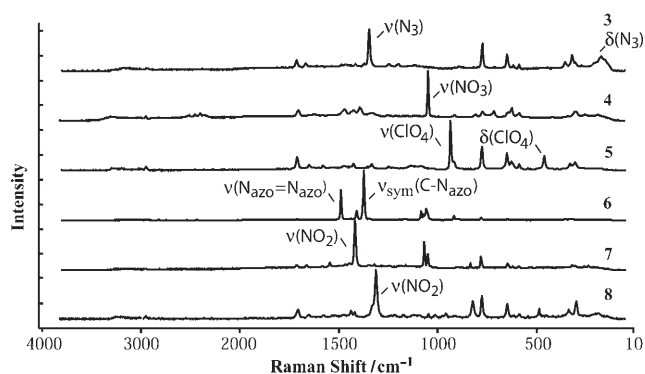


Figure 1. Panel plot of the Raman spectra of methylguanazinium energetic salts **3–8**.

tramide, $\nu(\text{NO}_2)$.^[35] The bands corresponding to the anions in the IR spectra (Figure 2) are observed at similar wavenumbers as in the Raman spectra: 1331 cm^{-1} (azide),

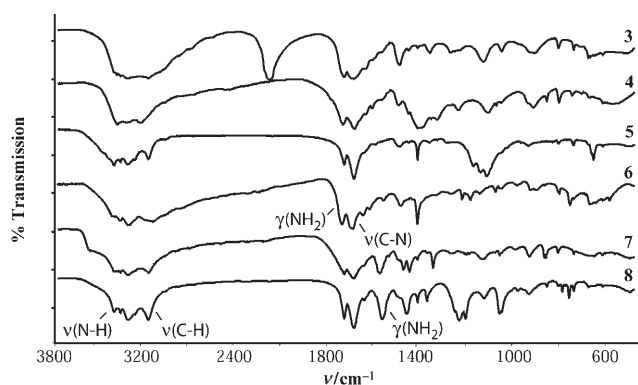


Figure 2. Panel plot of the IR spectra of energetic guanazinium salts **3–8**.

1046 cm^{-1} (nitrate), 907 cm^{-1} (perchlorate), 1385 and 1456 cm^{-1} (azotetrazolate), 1060 and 1419 cm^{-1} (nitrotetrazolate) and 1343 cm^{-1} (dinitramide). As can be seen in Figure 1, the Raman spectrum of the azotetrazolate salt and, to a lesser extent, that of the 5-nitrotetrazolate salt, is dominated by the C–N and $\text{N}_{\text{azo}}=\text{N}_{\text{azo}}$ stretching vibrations (**6**) and the nitro-group stretching and tetrazole ring deformation modes (**7**).

Due to the unavailability of methylguanazine, DFT calculations^[36] were performed on the parent guanazine; these results were used to facilitate assignment of the bands observed in the vibrational spectra. Table S1 in the Supporting Information contains the most important vibrational bands (in the IR and Raman spectra) observed for compounds **3–8** with their corresponding assignments. The IR spectra (Figure 2) are dominated by the N–H and C–H stretching bands at around $3200\text{--}3300$ and 3000 cm^{-1} , respectively. These bands have a complex shape depending on the mode of sample preparation and appear at very similar shifts for all salts except for nitrate **4**, indicating no significant difference in the strength of the hydrogen-bonding; that is, the

suspected extensive hydrogen-bonding due to the large number of hydrogen atoms available to interact with electronegative atoms is not reflected in the IR spectrum. This lack of extensive strong hydrogen-bonding is confirmed (in the solid state) by the X-ray measurements, which show weak hydrogen bonds for all salts and (in solution) by the ^{15}N NMR experiments in which a more substantial difference in the shifts caused by differences in hydrogen bonding would be expected (see discussion on ^{15}N NMR spectroscopy). The stretching modes of the $(\text{C}-\text{N})_{\text{ring}}$ and $(\text{N}-\text{N})_{\text{ring}}$ are observed as peaks of low intensity at $\nu \approx 1020$, 1425 , 1533 and 1580 cm^{-1} (IR).

The ^1H NMR spectra of the methylguanazinium salts in $[\text{D}_6]\text{DMSO}$ show three well-resolved signals for the amino-group protons for all salts, indicating slow proton exchange in the NMR solvent, at ≈ 8.0 (N-bound amino group), 6.5 and 5.7 ppm (C-bound amino groups), and one sharp peak at 3.4 ppm corresponding to the methyl group resonance. The resonances of the amino groups are shifted with respect to neutral guanazine^[23b] and protonated guanazinium salts,^[23,24] which, due to fast proton exchange, show two signals at ≈ 7.2 ($\text{N}-\text{NH}_2 + \text{C}-\text{NH}_2$) and ≈ 5.5 ppm ($\text{C}-\text{NH}_2$). In the ^{13}C NMR spectra, upon protonation of guanazine to form the guanazinium cation (GH^+),^[23] there is an upfield shift from 152.1 to ≈ 150.5 ppm in the triazolium-ring carbon-atom resonances.^[23–26] Similarly, upon methylation the two aromatic carbon atoms become unequivalent and one shows a resonance similar to GH^+ (≈ 151 ppm), whereas the ring-carbon atom closest to the methyl group experiences an upfield shift to ≈ 148 ppm. This is a similar effect to that observed in other nitrogen-containing heterocycles upon alkylation or protonation of the heterocyclic ring.^[26,37] The methyl group has a shift of ≈ 34 ppm, in keeping with compounds containing an *N*-methylated azole ring.^[31,37]

^{15}N NMR spectroscopy shows six signals for the six different nitrogen atoms in the cation (Figure 3). When the spec-

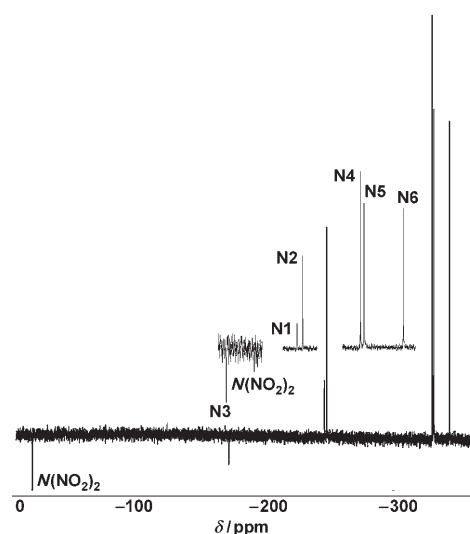


Figure 3. $^{15}\text{N}\{^1\text{H}\}$ NMR spectrum of the methylguanazinium cation in dinitramide salt **8**, measured in $[\text{D}_6]\text{DMSO}$.

trum is recorded with broadband decoupling, the resonances of the nitrogen atoms in close proximity to protons are strong and positive.^[24] All nitrogen atoms in the heterocyclic ring have positive signals due to the presence of hydrogen atoms at two bonds (either CH₃ or NH₂) apart from N3, which is at three bonds from the next proton, causing it to have a negative intensity. The resonances of the amino-group nitrogen atoms (at higher field) are well separated from those corresponding to the heterocyclic ring, which appear at lower field, but are very similar. The nitrogen-bound amino group (N4) would be expected to be found at lower field than the carbon-bound nitrogen atoms, due to the direct bond to the more electronegative nitrogen atom. The carbon-bound nitrogen atoms can be distinguished based on the methylation-induced shift (MIS) caused by the introduction of the methyl group onto guanazine. By comparison with neutral guanazine (Table 1), the nitrogen clos-

Table 1. ¹⁵N NMR shifts (δ [ppm]) in [D₆]DMSO for methylguanazinium salts **3–8** with N–H coupling constants (J [Hz]) in parentheses.

	N1	N2	N3	N4	N5	N6
1 ^[a]	–238		–156	–327	–340	
2 ^[b]	–238	–240	–163	–320 (80)	–322 (71)	–334 (72)
3	–239	–240	–165	–322 (75)	–322 (81)	–335 (85)
4	–239	–240	–165	–323 (76)	–324 (91)	–336 (87)
5	–239	–241	–165	–323 (76)	–324 (91)	–336 (88)
6	–239	–240	–165	–323 (79)	–323 (89)	–335 (88)
7	–238	–240	–164	–322 (76)	323 (86)	–335 (88)
8	–239	–240	–164	–322 (76)	–323 (92)	–336 (85)

[a] From reference [23b]. [b] From reference [26]

est to the methyl group (N6) would be expected to have the most negative MIS.^[31,37] In this case, both C–NH₂ groups have a positive shift of $\approx +17$ ppm (N5) and $\approx +5$ ppm (N6) and N6 (closest to the methyl group) can be assigned as having the resonance at the highest field. Taking advantage of the MIS observed, the assignment of N2 is straightforward (MIS ≈ -80 ppm), whereas the rest of the peaks remain practically unchanged by the methyl group and can be assigned by comparison to neutral guanazine.^[23] The amino-group nitrogen-atom resonances are observed at the highest field as three triplets: N4 and N5 overlap (Figure 3), whereas N6 has a slightly more negative shift. The coupling constants ($J(^1\text{H}-^{15}\text{N})$) have values of ≈ 75 –80 Hz (for N4) and ≈ 85 –90 Hz (for N5 and N6). The shifts mentioned above are in good agreement with iodide salt **2**,^[26] although the coupling constants to N5 and N6 are slightly larger for the compounds reported here (see Table 1). Apart from the cation, the nitrogen atoms belonging to the anion are also observed in the ¹⁵N NMR spectra. The dinitramide salt shows one resonance corresponding to the nitro groups at -11.1 ppm (N(NO₂)₂) and the central nitrogen atom resonates (with low intensity) at -177.8 ppm (N(NO₂)₂), similarly to other dinitramide salts.^[38] The nitrate nitrogen atom appears as an intense signal at -4.6 ppm, as expected.^[38] In contrast to other compounds with the same anion^[4,13a,57] the azotetrazolate salt (**6**) was soluble enough in [D₆]DMSO to

record a ¹⁵N NMR (natural abundance) spectrum and showed three well-resolved signals at $+107.5$ ppm, corresponding to the azo-bridge nitrogen atoms, and the ring resonances were observed at $+12.4$ (CN_α) and -66.5 ppm (CN_β), in keeping with the reported values for the resonances found in the solid-state NMR spectrum of guanazinium azotetrazolate^[24] and the solution-state NMR spectrum of the sodium salt.^[13a] Lastly, due to the high symmetry of the anion, the azide and 5-nitrotetrazolate resonances can be readily observed in the ¹⁴N NMR spectrum as broad signals at -130 (N/N) and -280 ppm (N/N)^[39–40] and at $\approx +20$ (N9/N10), -20 (NO₂) and -60 ppm (N8/N11),^[41] respectively.

Molecular structures: Single crystals of **3–8** suitable for X-ray diffraction studies were obtained as described in the Experimental Section. Intensity data were collected on an Oxford XCalibur 3 CCD diffractometer equipped with a molybdenum X-ray tube and a highly oriented graphite monochromator. The structures were solved by direct methods with SIR97^[42] and refined by means of full-matrix least-squares procedures with SHELXL-97.^[43] All non-hydrogen atoms were refined anisotropically by full-matrix least-squares methods. Details concerning data collection and refinement are summarised in Table 2. All hydrogen atoms were located from difference Fourier maps and were refined isotropically. CCDC-650180 (**3**), CCDC-650177 (**4**), CCDC-650724 (**5**), CCDC-650179 (**6**), CCDC-650725 (**7**) and CCDC-650178 (**8**) contain the supplementary crystallographic data for this paper. These data can be obtained free of charge from The Cambridge Crystallographic Data Centre via www.ccdc.cam.ac.uk/data_request/cif.

Selected bond lengths and angles in the methylguanazinium cations of the energetic salts synthesised are shown in Table 3. All parameters agree with each other, within experimental error,^[44] and match the reported data for the structure of the iodide salt.^[26] The formal exchange of the proton at N2 in guanazinium salts^[23,24,26] by a methyl group shows little variation in the molecular parameters found for the MeG⁺ ion in comparison to the GH⁺ ion or neutral guanazine.^[24] The triazolium ring is planar, with the exocyclic nitrogen atoms lying in this plane. The tetrahedral geometry and bond length (N1–N4 ≈ 1.40 Å) of the nitrogen-bound (N4) amino group indicates little interaction of the nitrogen lone-pair and the triazolium-ring π system, similar to other triazolium species,^[9,19,31,45] and as predicted by theoretical studies on *N*-aminoazoles, which led to the conclusion that sp³ hybridisation for N–NH₂ groups is preferred over sp² hybridisation.^[46] On the other hand, the carbon-bound amino groups (N5 and N6) have angles close to 120°, corresponding to a sp² hybridisation, and the C1–N6 and C3–N5 distances are in the range 1.317(4)–1.330(3) and 1.332(3)–1.357(2) Å, respectively. These distances are shorter than C–N single bonds (1.47 Å) and longer than C=N double bonds (1.22 Å),^[47] indicating a more accentuated conjugation of the nitrogen lone-pair with the heteroaromatic ring. In fact, a closer comparison of the C–NH₂ and N–NH₂ (1.393(2)–

Table 2. Crystallographic and refinement data for compounds **3–8**.

	3	4	5	6	7	8
formula	C ₃ H ₉ N ₉	C ₃ H ₉ N ₇ O ₃	C ₃ H ₉ N ₆ O ₄ Cl	C ₈ H ₂₀ N ₂₂ O	C ₄ H ₁₁ N ₁₁ O ₃	C ₃ H ₉ N ₉ O ₄
<i>M</i> _r [g mol ⁻¹]	171.16	191.15	228.60	440.39	261.20	235.16
crystal size [mm]	0.3 × 0.25 × 0.03	0.3 × 0.25 × 0.2	0.15 × 0.08 × 0.08	0.2 × 0.2 × 0.15	0.35 × 0.1 × 0.05	0.35 × 0.15 × 0.04
crystal system	monoclinic	triclinic	triclinic	triclinic	monoclinic	monoclinic
space group	<i>P</i> 2 ₁ / <i>c</i>	<i>P</i> $\bar{1}$	<i>P</i> $\bar{1}$	<i>P</i> $\bar{1}$	<i>P</i> 2 ₁ / <i>c</i>	<i>P</i> 2 ₁ / <i>c</i>
<i>a</i> [Å]	9.457(1)	5.318(1)	5.793(1)	7.741(5)	5.104(1)	9.8919(4)
<i>b</i> [Å]	17.418(1)	6.718(1)	7.613(1)	10.464(5)	13.233(1)	4.4530(2)
<i>c</i> [Å]	9.913(1)	11.236(3)	11.080(2)	12.074(5)	16.220(1)	21.4998(8)
α [°]	90	81.11(2)	83.12(1)	82.12(1)	90	90
β [°]	95.86(1)	86.44(2)	86.87(1)	88.46(1)	91.06(1)	95.32(1)
γ [°]	90	73.83(1)	69.61(2)	73.49(1)	90	90
<i>V</i> [Å ³]	1624.4(2)	380.9(2)	454.7(1)	928.7(8)	1095.4(2)	943.0(2)
<i>Z</i>	8	2	2	4	4	4
<i>T</i> [K]	200(2)	100(2)	200(2)	100(2)	100(2)	100(2)
ρ_{calcd} [g cm ⁻³]	1.399	1.667	1.669	1.575	1.584	1.657
μ [mm ⁻¹]	0.107	0.144	0.425	0.122	0.134	0.147
<i>F</i> (000)	720	200	236	460	544	488
θ range [°]	3.68–27.00	3.90–26.99	3.75–26.99	3.73–27.00	3.97–32.53	3.81–27.00
index ranges	–12 ≤ <i>h</i> ≤ 12 –22 ≤ <i>k</i> ≤ 22 –12 ≤ <i>l</i> ≤ 12	–6 ≤ <i>h</i> ≤ 6 –8 ≤ <i>k</i> ≤ 8 –14 ≤ <i>l</i> ≤ 14	–7 ≤ <i>h</i> ≤ 7 –9 ≤ <i>k</i> ≤ 9 –14 ≤ <i>l</i> ≤ 14	–9 ≤ <i>h</i> ≤ 9 –13 ≤ <i>k</i> ≤ 13 –15 ≤ <i>l</i> ≤ 14	–7 ≤ <i>h</i> ≤ 7 –19 ≤ <i>k</i> ≤ 19 –24 ≤ <i>l</i> ≤ 24	–12 ≤ <i>h</i> ≤ 12 –5 ≤ <i>k</i> ≤ 5 –27 ≤ <i>l</i> ≤ 27
reflns collected	16 405	8544	4932	9549	15 103	8842
independent reflns	3539	1668	1968	3794	2046	2046
<i>R</i> _{int}	0.0818	0.0271	0.0282	0.0504	0.0581	0.0577
parameters	277	154	163	360	207	181
<i>S</i> on <i>F</i> ²	1.040	1.100	1.103	1.027	1.007	1.065
<i>R</i> ₁ [<i>F</i> > 2σ(<i>F</i>)] ^[a]	0.0632	0.0343	0.0416	0.0363	0.0433	0.0440
<i>wR</i> ₂ (all data) ^[b]	0.1463	0.1008	0.1220	0.1319	0.1118	0.1015

[a] $R_1 = \sum ||F_o| - |F_c|| / \sum |F_o|$. [b] $wR_2 = [\sum (F_o^2 - F_c^2) / \sum w(F_o^2)]^{1/2}$.

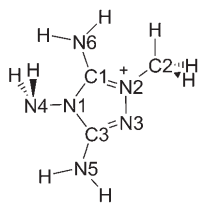
1.407(3) Å) distances in compounds **3–8** with the C–N and N–N distances in CH₂=NH/CH₃–NH₂ (1.273 and 1.471 Å) and NH=NH/NH₂–NH₂ (1.252 and 1.449 Å), respectively,^[48] further supports this observation and shows the “hydrazine-like” character of the amino group in the 1-position (N4) and the “aniline-like” character of the carbon-bound amino groups (N5 and N6). Salts **3**, **7** and **8** crystallise in monoclinic systems in the space-group *P*2₁/*c* with four molecules in the unit cell (apart from **3**, *Z*=8), whereas **4**, **5** and **6** have triclinic cells in the space-group *P* $\bar{1}$, with *Z*=2. By using graph-set notation^[49] and the computer program RPLUTO,^[50] the hydrogen-bond patterns of interest can be identified and analysed. Common to all structures is the formation of an intramolecular hydrogen bond, which describes an **S(5)** motif at the primary level. The intramolecular hydrogen bond is formed between the C–NH₂ group nearest to the methyl residue (N6, donor) and the N–NH₂ group (N4, acceptor) in the case of **3**, **6** and **7**, and between the C–NH₂ group furthest from the methyl residue (N5, donor) and the N–NH₂ group (N4, acceptor) in the case of **4**, **5**, and **8**, and has a length of ≈2.85 Å. In addition, the formation of a hydrogen bond between N5 (donor) of one triazolium cation and N3 (acceptor) of another cation, gives rise to the formation of an **R₂²(8)** motif with N5⋯N3 ≈3 Å. The dinitramide salt is the only compound that does not show such a motif (see discussion below).

The asymmetric unit of compound **3** (Figure 4) contains two crystallographically independent anions and cations. The cations have very similar geometric parameters between

them and with the other salts. Also the azide anions are very similar, essentially linear (N–N–N ≈179°) and symmetrical around the central nitrogen (N02 or N05) with N–N distances of ≈1.17 Å, typical for N=N double bonds^[51] and similar to other azolium azides.^[39,45]

While the cations arrange forming layers perpendicular to the *ac* plane, one of the crystallographically independent azide anions lies approximately in this plane (angle between N1, N3 and the *ac* plane ≈15°) and the other lies crossing these layers at an angle of ≈50°. The more out-of-the-plane azide anion connects three consecutive layers through two hydrogen bonds with the terminal nitrogen atoms (N4⋯N06ⁱⁱ = 3.038(4) Å; N10⋯N04 = 3.028(4) Å, symmetry code: ii: –*x*, –*y*+1, –*z*+1), whereas the other anion forms a hydrogen bond with the twisted nitrogen-bound amino group in the cation linking layers (N10⋯N03^{iv} = 2.994(5) Å, symmetry code: iv: *x*–1, *y*, *z*). In each layer (Figure 5), both azide anions are involved in hydrogen-bonding at the terminal nitrogen atoms (N6^{viii}⋯N06^{ix}, 2.923(3) Å; N6⋯N01, 2.893(4) Å; N12⋯N01ⁱⁱⁱ, 2.861(4) Å; N12⋯N06^{vi}, 2.968(4) Å; N11⋯N03^{vii}, 2.815(4) Å; N5⋯N04, 2.913(4) Å; symmetry codes: iii: *x*–1, –*y*+1/2, *z*+1/2; v: *x*, –*y*+1/2, *z*+1/2; vi: –*x*–1, –*y*+1, –*z*+1; vii: –*x*, –*y*+1, –*z*; viii: 1–*x*, *y*+1/2, –*z*+1/2; ix: 1+*x*, *y*, *z*). One azide anion participates in the formation of four hydrogen bonds (see Table S2 in the Supporting Information), three within a layer and one between layers, whereas the other azide anion forms three hydrogen bonds within a layer and two between layers. The lines of cations are connected by hydrogen bonding through “azide

Table 3. Selected bond lengths [Å] and angles [°] for the methylguanazinium cation in salts **3–8**.



Parameter	3		4	5	6		7	8
	A	B			A	B		
N2–C1	1.323(3)	1.322(3)	1.314(2)	1.321(3)	1.320(2)	1.326(2)	1.328(2)	1.313(2)
N2–N3	1.409(3)	1.406(3)	1.404(2)	1.409(3)	1.411(2)	1.415(2)	1.409(2)	1.410(2)
N2–C2	1.446(4)	1.445(4)	1.443(2)	1.443(4)	1.447(2)	1.448(2)	1.445(2)	1.459(3)
N3–C3	1.305(3)	1.306(3)	1.306(2)	1.309(3)	1.309(2)	1.305(2)	1.320(2)	1.314(3)
N5–C3	1.343(4)	1.347(4)	1.333(2)	1.332(3)	1.352(2)	1.357(2)	1.340(2)	1.335(3)
N1–C1	1.358(3)	1.355(3)	1.356(2)	1.352(3)	1.358(2)	1.361(2)	1.354(2)	1.363(3)
N1–C3	1.378(3)	1.382(3)	1.377(2)	1.378(3)	1.380(2)	1.379(2)	1.385(2)	1.374(3)
N1–N4	1.405(3)	1.402(3)	1.399(2)	1.399(3)	1.398(2)	1.393(2)	1.399(2)	1.399(2)
N6–C1	1.325(4)	1.317(4)	1.323(2)	1.320(3)	1.322(2)	1.324(2)	1.318(2)	1.330(3)
C1–N2–N3	111.3(2)	111.4(2)	111.4(1)	111.4(2)	110.8(1)	110.8(1)	111.2(2)	111.7(2)
C1–N2–C2	128.8(2)	128.8(3)	127.8(1)	128.0(2)	129.2(1)	128.1(1)	127.2(2)	129.3(2)
N3–N2–C2	119.7(2)	119.7(2)	120.6(1)	120.2(2)	120.0(1)	119.9(1)	121.5(2)	118.9(2)
C3–N3–N2	103.8(2)	103.9(2)	104.0(1)	104.0(2)	104.3(1)	104.2(1)	104.0(2)	103.6(2)
C1–N1–C3	107.1(2)	107.3(2)	107.2(1)	108.0(2)	107.2(1)	107.2(1)	107.4(2)	107.5(2)
C1–N1–N4	121.8(2)	122.5(2)	128.7(1)	128.1(2)	122.0(1)	122.6(1)	122.9(2)	128.9(2)
C3–N1–N4	131.0(2)	130.2(2)	124.0(1)	123.8(2)	130.8(1)	130.2(1)	129.6(2)	123.6(2)
N3–C3–N5	126.7(3)	125.9(3)	127.0(1)	127.8(2)	127.0(1)	127.5(1)	127.2(2)	127.7(2)
N3–C3–N1	111.4(2)	111.0(2)	110.9(1)	110.6(2)	110.8(1)	111.3(1)	110.6(2)	111.0(2)
N5–C3–N1	121.9(3)	123.0(3)	122.1(1)	121.6(2)	122.1(1)	121.1(1)	122.1(2)	121.4(2)
N2–C1–N6	129.0(3)	129.3(3)	127.8(1)	128.1(2)	128.4(2)	129.1(2)	128.3(2)	130.2(2)
N2–C1–N1	106.3(2)	106.2(2)	106.4(1)	106.0(2)	106.8(1)	106.5(1)	106.7(2)	106.2(2)
N6–C1–N1	124.7(3)	124.5(3)	125.7(1)	125.8(2)	124.7(1)	124.4(1)	125.0(2)	123.6(2)

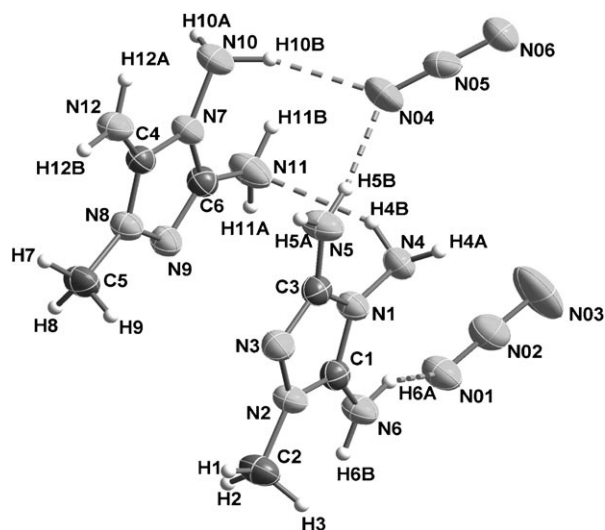


Figure 4. Asymmetric unit of methylguanazinium azide (**3**) showing the numbering scheme (Diamond plot, thermal ellipsoids represent 50% probability).

bridges” and by direct hydrogen-bond interactions between the cations (N11 \cdots N3ⁱ 2.956(4) Å; N5 \cdots N9^v 3.009(4) Å; symmetry codes: i: $x, -y+1/2, z-1/2$; v: $x, -y+1/2, z+1/2$) forming a two-dimensional network. The side-on interaction

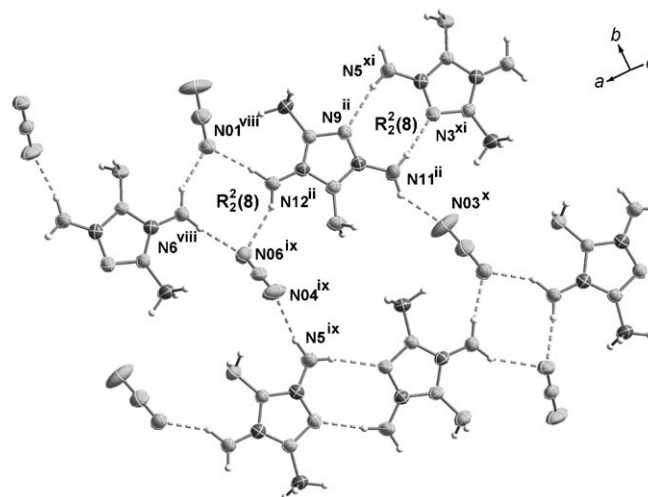


Figure 5. Hydrogen bonding within a layer of **3** (symmetry codes: ii: $-x, -y+1, -z+1$; viii: $1-x, y+1/2, -z+1/2$; ix: $1+x, y, z$; x: $x, y, z+1$; xi: $-x, y+1/2, -z+3/2$).

of triazole rings results in the formation of the usual **R₂(8)** motif. It is interesting to note the formation of another **R₂(8)** subset by the aforementioned “azide-bridged” triazoles, as observed for other azolium azides.^[37] The formation of extensive strong hydrogen bonding within a layer and be-

tween layers would suggest a high density in the crystal structure of the compound; however, a moderate value of $\approx 1.4 \text{ g cm}^{-3}$ was calculated. This value is similar to that of previously reported 1,4-dimethyl-5-aminotetrazolium azide (DMATA),^[37] which, due to the presence of the two methyl groups, has many fewer protons available for hydrogen bonding. The fairly low value indicates that there are many other factors that determine the density of a material in addition to hydrogen-bonding interactions. The low packing efficiency of **3**, caused by one of the two crystallographically independent azide anions that deviates from the plane formed by the triazolium rings, may explain the similar density to DMATA, which forms perfectly planar layers.

Compound **4** (Figure 6) crystallises in layers in which the nitrate anion is twisted slightly out of the plane formed by the methylguanazinium cations. The distances between

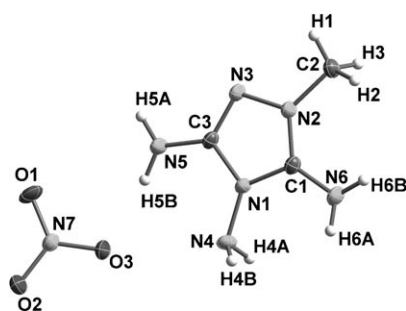


Figure 6. Asymmetric unit of methylguanazinium nitrate (**4**) showing the numbering scheme (Diamond plot, thermal ellipsoids represent 50% probability).

layers are $\approx 3.2 \text{ \AA}$ (measured between the twisted N4H_2 amino group and the nitrate nitrogen atom N7^{ii} from a neighbouring layer, symmetry code: ii: $1+x, y, z$) and the out-of-the-plane oxygen atom (O3) connects the layers by forming a hydrogen bond with the twisted N4H_2 , with a distance between donor and acceptor ($\text{N4}\cdots\text{O3}^{\text{iii}}$) of $3.026(2) \text{ \AA}$. In addition, O2 in the nitrate also links the layers by forming a hydrogen bond with the other hydrogen atom on N4 (H4A), with a distance ($\text{N4}\cdots\text{O2}$) of $3.113(2) \text{ \AA}$.

Cations and anions alternate forming extensive hydrogen bonding within a layer as represented in Figure 7. Every guanazinium cation is surrounded by three anions and one cation forming strong hydrogen bonds (see Table S3 in the Supporting Information for hydrogen-bond parameters). The $\text{R}_2^2(8)$ subset is formed by two consecutive guanazinium cations ($\text{N5}\cdots\text{N3}^{\text{iii}} = \text{N5}^{\text{iii}}\cdots\text{N3} = 3.019(2) \text{ \AA}$; symmetry code: iii: $1-x, -y, 1-z$) at the primary level. Many other ring patterns are also formed. The most representative is another $\text{R}_2^2(8)$ subset, which is formed by a strong interaction between two cations and two anions ($\text{N6}\cdots\text{O2}^{\text{i}} = 2.818(2) \text{ \AA}$, $\text{N6}\cdots\text{O2}^{\text{iv}} = 2.893(3) \text{ \AA}$, symmetry codes: i: $1-x, -y, 2-z$; iv: $2+x, -1+y, z$), well below the sum of the van der Waals radii ($r_{\text{O}} + r_{\text{N}} = 3.10 \text{ \AA}$)^[52] and a larger $\text{R}_2^2(14)$ motif, again by interaction of two guanazinium cations with two nitrate anions ($\text{N4}\cdots\text{O3}^{\text{ii}} = 3.026(2) \text{ \AA}$, $\text{N5}\cdots\text{O3} = 2.911(2) \text{ \AA}$, symme-

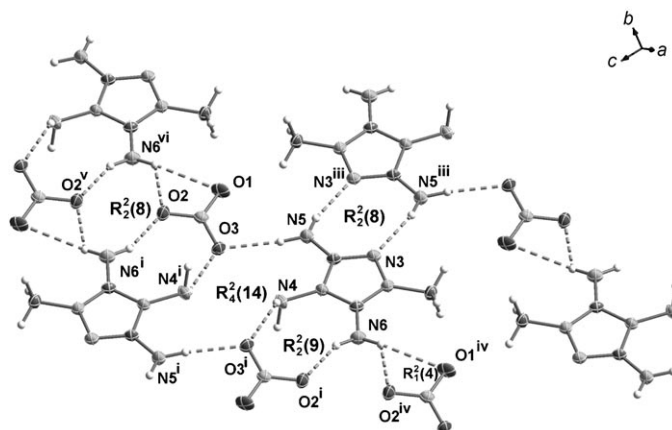


Figure 7. View of one of the layers showing the extensive hydrogen bonding in **4** (symmetry codes: i: $1-x, -y, 2-z$; iii: $1-x, -y, 1-z$; iv: $2+x, -1+y, z$; v: $-1-x, 1-y, 2-z$; vi: $-2+x, 1+y, z$).

try code: ii: $x+1, y, z$). Additionally, the $\text{R}_2^2(4)$ ring pattern, common to nitrate salts, is also found with one weak interaction ($\text{N6}\cdots\text{O1}^{\text{iv}} = 3.312(2) \text{ \AA}$) and one strong one ($\text{N6}\cdots\text{O2}^{\text{iv}} = 2.893(2) \text{ \AA}$). The parameters corresponding to the anion are as observed for many other nitrate salts^[45,53,54] and will not be further discussed.

The perchlorate anion in **5** is linked to five cations through hydrogen-bonding (Figure 8). The O3 and O4 oxygen atoms form two hydrogen bonds each ($\text{N4}^{\text{iv}}\cdots\text{O3}$

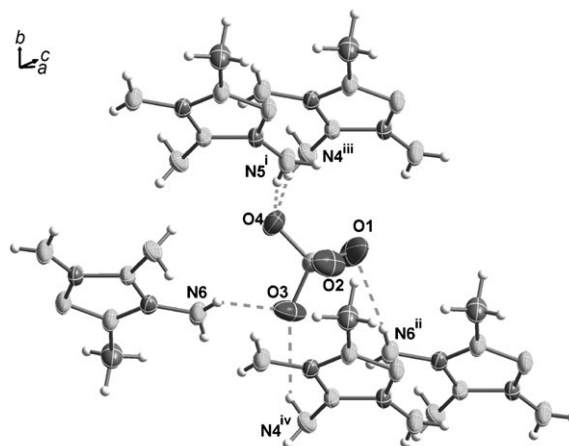


Figure 8. Hydrogen bonding around the perchlorate anion in **5** (symmetry codes: i: $-1-x, 1-y, 1-z$; ii: $1-x, -y, 1-z$; iii: $-x, 1-y, 1-z$; iv: $-x, -y, 1-z$).

$3.042(3) \text{ \AA}$, $\text{N6}\cdots\text{O3} = 2.943(4) \text{ \AA}$ and $\text{N4}^{\text{iii}}\cdots\text{O4} = 3.111(3) \text{ \AA}$, $\text{N5}\cdots\text{O4} = 3.198(4) \text{ \AA}$) whereas O1 forms only one ($\text{N6}^{\text{ii}}\cdots\text{O1} = 3.055(4) \text{ \AA}$) and O2 does not form any (symmetry codes: i: $-1-x, 1-y, 1-z$; ii: $1-x, -y, 1-z$; iii: $-x, 1-y, 1-z$; iv: $-x, -y, 1-z$).

Three consecutive layers are connected by hydrogen bonds (Table S4 in the Supporting Information) with the nitrogen-bound amino group, once with O3 and once with O4

of the perchlorate anion ($N4^{vi}\cdots O3$, 3.042(3) Å and $N4^{viii}\cdots O4$, 3.111(3) Å; symmetry codes: vi: $-x, -y, 1-z$, viii: $-1-x, 1-y, 1-z$). Figure 9 shows one of the layers in the

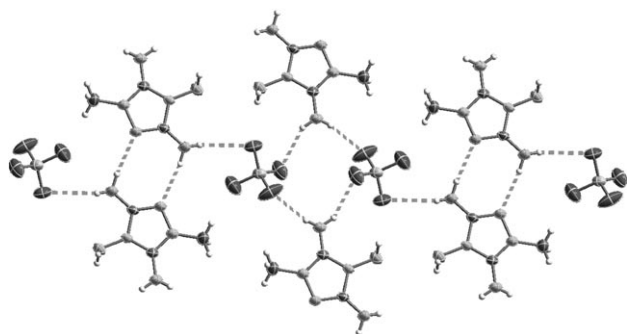


Figure 9. View of one of the cations layers in **5** (symmetry codes: iv: $-x, -y, 1-z$; vi: $-x, -y, 1-z$; $-2-x, 1-y, 1-z$; viii: $-1-x, 1-y, 1-z$).

structure. $R_2^2(8)$ motifs alternate with the much less common $R_2^2(12)$ subsets. The latter are analogous to the $R_2^2(8)$ motifs formed by the azide bridges in **3**, only in this case the perchlorate anions bridge the two cations through the oxygen atoms ($N6\cdots O3$ 2.943(4) Å, $N6\cdots O1^{ii}$ 3.055(4) Å; symmetry code: ii: $1-x, -y, 1-z$) increasing the size of the hydrogen-bonded ring pattern from 8 (in the azide salt) to 12 (in the perchlorate salt). The perchlorate anion distances and angles are in agreement with other salts of perchloric acid with amines.^[45,53,54]

The tetrazole rings in the anion of **6** are not equivalent due to the presence of one molecule of water in the crystal structure (Figure 10). The azo bridge distance ($N17-N18$), with a value of 1.26 Å, is comparable to that observed in metal azotetrazolates^[13a] and hydrazinium azotetrazolate^[55] and longer than the reported bond length of 1.20 Å for bis[hydroxolead(II)] 5,5'-azotetrazolate.^[56] The angles in the anion are all similar to comparable compounds.^[13a,55] The

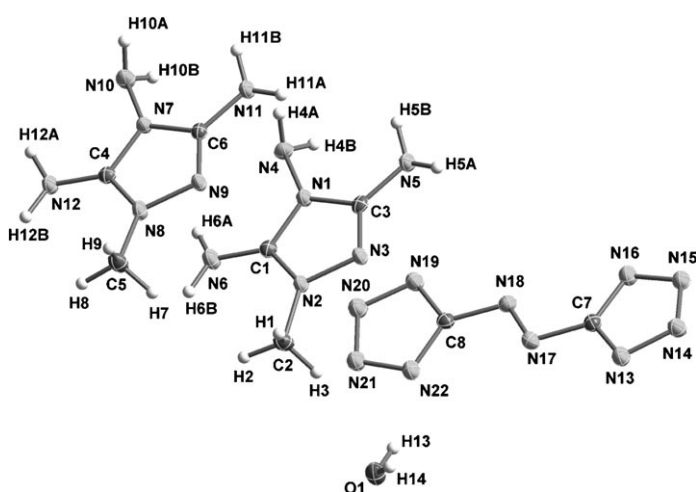


Figure 10. Asymmetric unit of methylguanazinium 5,5'-azotetrazolate monohydrate (**6**) showing the numbering scheme (Diamond plot, thermal ellipsoids represent 50% probability).

nonplanar amino group joins the slightly wavy layers through hydrogen bonding to the azotetrazolate anions ($N10\cdots N16^{ii}$, 3.062(3) Å; symmetry code: ii: $1-x, 1-y, 1-z$). The other crystallographically independent cation uses both hydrogen atoms of the most off-the-plane amino group to link to the amino group of a cation of the layer below ($N4\cdots N5^{ii}$, 3.191(3) Å) and one of the layer above ($N4\cdots N11$, 3.140(3) Å). Furthermore, water molecules build two types of hydrogen bonds of similar strengths (≈ 2.93 Å), once to the anion and once to one of the carbon-bound amino groups in the cation.

Figure 11 shows the hydrogen bonding around the anion in **6** (see Table S5 in the Supporting Information for distances and angles). Every nitrogen atom in the anion is

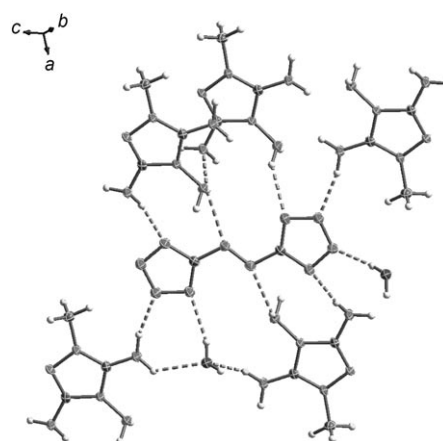


Figure 11. Hydrogen-bonding around the azotetrazolate anion in **6** (symmetry codes: i: $x, y, 1+z$; ii: $1-x, 1-y, 1-z$; iii: $2-x, 1-y, 1-z$; iv: $1+x, -1+y, 1+z$; v: $2-x, -y, 1-z$; vi: $2-x, 1-y, -z$; vii: $x, y, -1+z$; viii: $-1+x, 1+y, -1+z$).

involved in hydrogen bonding apart from N20. A total of five guanazinium cations and two water molecules complete the coordination around the anion. Two of the cations form two hydrogen bonds: one to the azo nitrogen atom N17 ($N18$) and one to the tetrazole ring nitrogen N13 ($N19$) atoms with distances between donor and acceptor at $N10\cdots N17^i = 3.082(2)$ Å ($N4\cdots N18^{ii} = 3.073(3)$ Å) and $N11\cdots N13^i = 3.034(2)$ Å ($N5\cdots N19^{ii} = 2.925(2)$ Å, symmetry codes: i: $x, y, 1+z$; ii: $1-x, 1-y, 1-z$). Consecutive cations are connected by hydrogen bonds with water molecules ($N6\cdots O1^v = 2.862(2)$ Å and $N12\cdots O1^i = 2.927(2)$ Å; symmetry code: v: $2-x, -y, 1-z$). In addition, the extensive hydrogen bonding in the structure, not only within a layer but also between layers, may account for the relatively high density of the azotetrazolate salt ($\rho_{\text{calc}} = 1.57 \text{ g cm}^{-3}$) compared to other ionic compounds with the same anion, which have densities of $\approx 1.45 \text{ g cm}^{-3}$.^[52,57] Lastly, one $R_2^2(7)$ and one $R_2^2(12)$ subsets are formed between one cation, one anion and one molecule of water.

Compound **7** crystallises with one water molecule in the unit cell (Figure 12) in a layered structure in which the

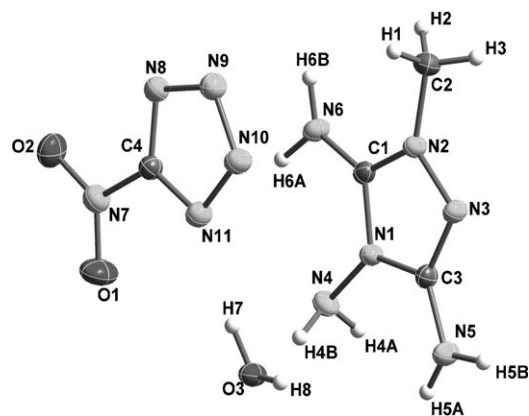


Figure 12. Asymmetric unit of methylguanazinium 5-nitrotetrazolate monohydrate (**7**) showing the numbering scheme (Diamond plot, thermal ellipsoids represent 50% probability).

water molecules link two consecutive layers by hydrogen bonding to the out-of-plane nitrogen-bound amino group ($N4 \cdots O3$, 2.986(2) Å). Figure 13 shows the hydrogen-bond-

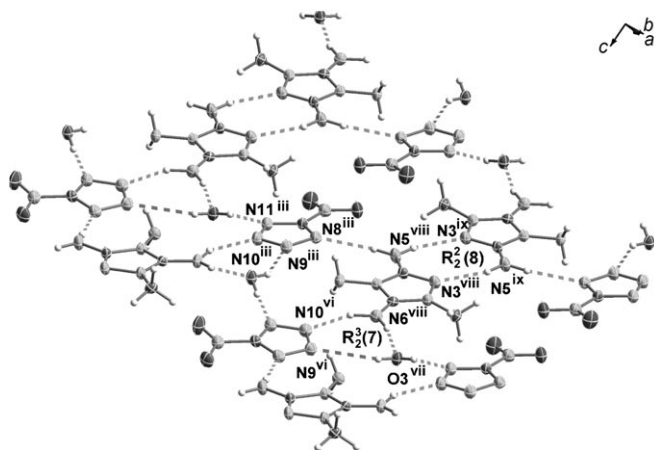


Figure 13. View of a layer with the corresponding hydrogen-bonding in **7** (symmetry codes: iii: $1-x, 0.5+y, 1.5-z$; vi: $-1+x, 1+y, z$; vii: $1-x, 1.5+y, 1.5-z$; viii: $x, 1+y, z$; ix: $2-x, 1-y, 1-z$).

ing in one of these layers. Cations and anions alternate in the b direction. The nitro groups of two nitrotetrazolate anions are oriented head-on, and water molecules connect the anions through one strong and one weak hydrogen bond ($O3 \cdots N11$ 2.808(2) Å, $O3 \cdots N9^v$ 3.256(2) Å; symmetry code: v: $2-x, -0.5+y, 1.5-z$). All nitrogen atoms in the nitrotetrazolate ring are involved in hydrogen bonding to either one of the aforementioned bridging water molecules or to the carbon-bound amino groups of the cation ($N6 \cdots N10^i$, 2.901(2) Å; $N5 \cdots N8^{iv}$, 3.125(2) Å; symmetry codes: i: $-1+x, y, z$; iv: $1-x, -0.5+y, 1.5-z$). The atoms N5 and N3ⁱⁱ form a $R_2^2(8)$ motif at the primary level ($N5 \cdots N3^{ii} = 2.977(2)$ Å; symmetry code: ii: $2-x, -y, 1-z$) and one cation (N6), one anion (N9ⁱ and N10^o) and one water molecule (O3ⁱⁱⁱ) participate in the formation of a $R_2^3(7)$ subset. Every hydrogen

atom of the three amino groups in the guanazinium moiety also forms hydrogen bonds, which link every cation to two cations, two anions, and two water molecules (see Table S6 in the Supporting Information for distances). The atoms N5 (in the cation) and N8^{iv} (in the anion) form a very directional contact with $N5-H5A-N8^{iv} = 175^\circ$. The tetrazolate anion is, within the limits of error, symmetrical with a symmetry plane, which runs along N7, C4 and cuts in the mid-point of the bond formed by N9 and N10 as reported for salts containing the same anion.^[58,59]

The asymmetric unit of **8** is shown in Figure 14. The overall geometry of the anion is similar to that observed in comparable dinitramide salts.^[60–62] The two N–N bond lengths

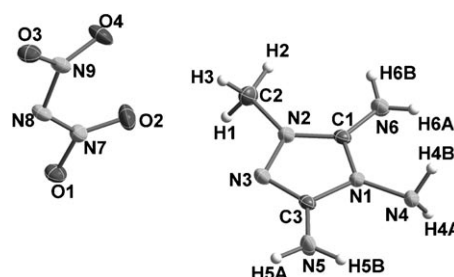


Figure 14. Asymmetric unit of methylguanazinium dinitramide (**8**) showing the numbering scheme (Diamond plot, thermal ellipsoids represent 50% probability).

are approximately symmetric (≈ 1.38 Å) and shorter than a normal N–N single bond (1.454 Å), though longer than a N=N double bond (1.245 Å).^[47] The N–N–N angle is 115.1(2)° as expected. The nitro groups are twisted out of the N–N–N plane (torsion angle $O2-N7-N9-O4 = 16.4(2)^\circ$) making the local symmetry of the anion C_1 .

Figure 15 shows a view of the hydrogen bonding in the crystal structure of **8**. Apart from the aforementioned intramolecular hydrogen bond ($N5 \cdots N4$, 2.841(3) Å), there are many different strong hydrogen bonds that make the structure relatively dense ($\rho_{\text{calcd}} = 1.656 \text{ g cm}^{-3}$) in comparison to other dinitramide salts.^[37,62] Every guanazinium cation forms

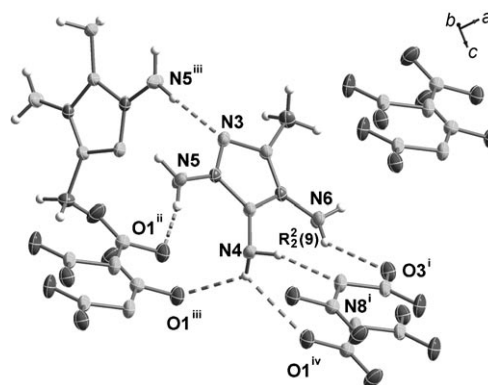
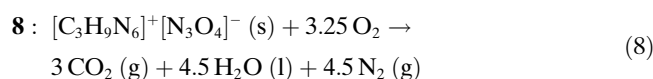
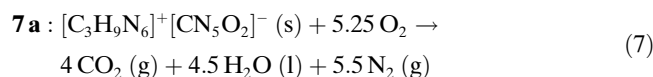
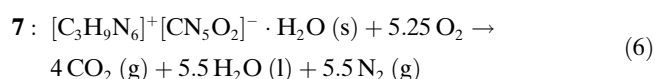
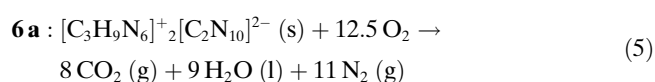
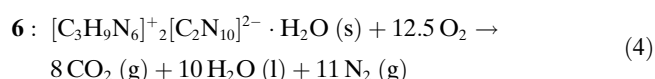
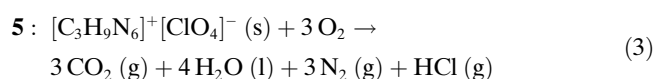
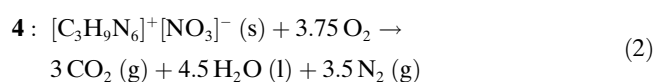
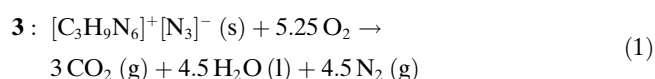


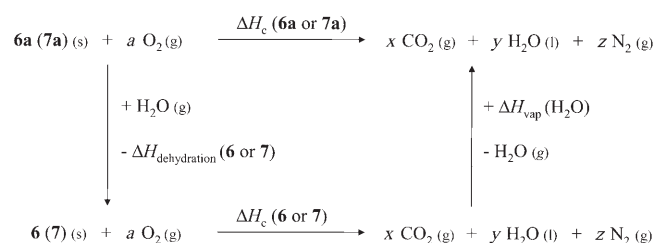
Figure 15. Hydrogen bonds in **8** (symmetry codes: i: $x, 1.5-y, 0.5+z$; ii: $-x, 0.5+y, 0.5-z$; iii: $-x, -0.5+y, 0.5-z$; iv: $x, 0.5-y, 0.5+z$).

up to eight hydrogen bonds, six to the anion and two to another cation. The dinitramide salt is, among the guanazinium salts studied here, the only compound that does not form the common $R_2^2(8)$ subset described above. The N3 atom interacts through a hydrogen bond with $N5^{iii}$ ($N3 \cdots N5^{iii}$, 2.966(3) Å; symmetry code: iii: $-x, -0.5+y, 0.5-z$), as expected, but there is no interaction between N5 and $N3^{iii}$. The lack of formation of this commonly observed motif, might be the result of packing effects in the crystal, which force, in contrast to iodide $2^{[26]}$ and salts **3–7**, two contiguous cations not to be coplanar. In the anion, O2 and O4 do not participate in hydrogen bonding, whereas O3 forms two hydrogen bonds ($N6 \cdots O3^i$, 3.068(2) Å and $N6 \cdots O3^{iv}$, 2.851(2) Å; symmetry codes: i: $x, 1.5-y, 0.5+z$; iv: $x, 0.5-y, 0.5+z$) and O1 up to three (see Table S7 in the Supporting Information). The central nitrogen atom in the anion also interacts with N4 of the cation ($N4 \cdots N8^i$, 3.041(2) Å). There are many other hydrogen-bond ring patterns, which one would expect for **8**; however, since the compound does not form layers, the formation of hydrogen bonds around the cation takes place with two anions located at different planes, preventing the formation of, for example, the expected $R_1^2(4)$ subset (common to compounds containing the NO_2 moiety such as nitrate **4**). The only ring pattern observed ($R_2^2(9)$) is formed by N4 and N6 (from the cation) and $N8^i$ and $O3^i$ (from the anion) with $N4 \cdots N8^i = 3.041(2)$ Å and $N6 \cdots O3^i = 3.068(2)$ Å, respectively.

Physical and energetic properties: To assess the energetic properties of compounds **3–8**, the thermal stability (melting and decomposition points from DSC measurements), and sensitivity to impact, friction,^[63–65] and thermal shock of each salt was experimentally determined. In addition, the constant pressure heats of combustion (ΔH_{comb}) of each salt were calculated from the predicted heats of reaction (ΔH_r) and an approximation of lattice enthalpy using the corresponding combustion equations [Eq. (1)–(8)].



The electronic energies for all anions and the methylguanazinium cation were calculated by using Møller–Plesset perturbation theory truncated at the second-order (MP2) and were used unscaled. The results of the MP2 electronic energy calculations are given in Table S8 in the Supporting Information. For all atoms in all calculations, the correlation consistent polarised double-zeta basis set cc-pVDZ was used. For compounds **6** and **7**, which form as monohydrates, the following approximation was used: the calculated (MP2 method) electronic energies were used to predict the heats of combustion of the anhydrous compounds **6a** and **7a** assuming that $\Delta H_{hydration} \ll \Delta H_c$ in the Born–Haber cycle shown in Scheme 2. The unit cell volume (V) for **6a** and **7a**



Scheme 2. Born–Haber energy cycle for the calculation of the heat of combustion of **6a** and **7a** (**6**: $a=12.5, x=8, y=10, z=11$; **6a**: $a=12.5, x=8, y=9, z=11$; **7**: $a=5.25, x=4, y=5.5, z=5.5$ and **7a**: $a=5.25, x=4, y=4.5, z=5.5$).

was approximated as being that of the monohydrate compounds minus the volume of the number of water molecules in the unit cell ($V(H_2O) = 0.02496 \text{ nm}^3$).^[67] Since the temperatures of water loss (DSC) for compounds **6** and **7** are relatively close to 100 °C, it is assumed that the interactions in the crystal structure are similar enough to those found in liquid water and the above approximation is valid. Typical values for hydration energies in similar compounds have values of about -20 cal g^{-1} and are smaller than 1% of the combustion energies.^[57b] In addition, errors in the combustion measurements are estimated at $\approx 5\%$; therefore, disregarding the hydration enthalpy is justified. On the other hand, the volume of the unit cell has little effect on the predicted values (errors of $\approx 5\%$ in the volume produce errors of $\approx 2\%$ in the calculated energies of formation). In addition, the energies of formation calculated for the anhydrous species **6a** and **7a** were used to calculate their detonation parameters by using the (X-ray) densities of the monohydrate salts **6** and **7**. This is justified by our experience that crystal water has generally little effect on the density values.^[57,68] Lastly, a similar method to the one used here has already been described before.^[68,69]

DSC studies on small samples of the materials show a family of salts with high thermal stability ($T_{\text{decomp}} > 200^\circ\text{C}$, except for **7** and **8**), possibly attributable to the high thermal stability of the methylguanazinium cation itself and extensive hydrogen bonding in the solid state. Comparison of the melting points and decomposition temperatures of the iodide salt (**2**)^[26] with the new compounds **3–8** (Tables 4 and 5) clearly illustrates the influence of the different anions, that is, the melting points follow the order nitrate > perchlorate > azide (> azotetrazolate) > nitrotetrazolate > dinitramide. A similar trend is observed for the decomposition temperatures: perchlorate > nitrate > azide > azotetrazolate > nitrotetrazolate > dinitramide. Compounds **3** and **4** melt with concomitant decomposition, whereas **6** decomposes without melting. On the other hand, **7** and **8** have decomposition points that are $\approx 30^\circ\text{C}$ above their melting points and the perchlorate salt (**5**) has the best thermal stability, decomposing at $> 300^\circ\text{C}$. Trends in the melting and decomposition temperatures observed are in agreement with our previous report on 1,4-dimethyl-5-aminotetrazolium (DMAT⁺) perchlorate, nitrate, azide and dinitramide salts,^[37] with the exception of the nitrate salt (**4**), which has an expectedly high melting point at 258°C , much higher than DMAT⁺ nitrate ($T_{\text{m}} = 181^\circ\text{C}$). This may be due to hydrogen bonding and packing effects, which are also reflected in the higher density of **4** (1.667 vs. 1.523 g cm^{-3}) or the nature of the MeG⁺ ion itself, since according to this and previous studies^[23b,24,26a] guanazinium salts tend to have liquid ranges of only a few degrees (if at all). Lastly, the decomposition points are in keeping with known heterocycle-based salts^[37,58] and approximately (except for **8**) in the range between that of RDX (230°C) and TNT (300°C).

In addition to DSC analysis, the response of each compound to fast thermal shock was tested by placing a small sample of the material in the flame. Apart from compounds **4** and **7** that burn normally, the rest deflagrate in the flame (both TNT and RDX explode under similar conditions). From these results it would seem like salts with a high nitrogen content such as **3** and **6**, or a better (less negative) oxygen balance (**5** and **8**) are more sensitive to fast heating.

Data collected for impact, friction and electrostatic discharge sensitivities are summarised in Table 6 together with the calculated (EXPLO5) detonation parameters. Only compounds **5** (25 J) and **8** (20 J) are slightly sensitive to shock, whereas the rest of the compounds are insensitive ($> 40\text{ J}$). The friction sensitivity values for **3–8** are also very low ($> 320\text{ N}$) except for perchlorate **5** (220 N), which can be classified as a sensitive material according to the UN Recommendations on the Transport of Dangerous Goods.^[64] A comparison of these values to those

measured for TNT and RDX is useful to assess the energetic salts in this study. All compounds are less sensitive to

Table 4. Physicochemical properties of methylguanazinium salts **3–5** and **8**.

	3	4	5	8
formula	$\text{C}_3\text{H}_9\text{N}_9$	$\text{C}_3\text{H}_9\text{N}_7\text{O}_3$	$\text{C}_3\text{H}_9\text{N}_6\text{O}_4\text{Cl}$	$\text{C}_3\text{H}_9\text{N}_9\text{O}_4$
M_r [g mol^{-1}]	171.16	191.15	228.61	235.16
T_{m} [$^\circ\text{C}$] ^[a]	212	258	247	129
T_{d} [$^\circ\text{C}$] ^[b]	215	261	310	160
N [%] ^[c]	73.6	51.3	36.8	53.6
$N + O$ [%] ^[d]	73.6	76.4	64.7	80.8
Ω [%] ^[e]	-98.1	-62.8	-42.0	-44.2
ρ [g cm^{-3}] ^[f]	1.399	1.667	1.669	1.657
ΔH_{comb} [cal g^{-1}] ^[g]	-4186	-3165	-2873	-2788
$\Delta U_{\text{c}}^\circ$ [kJ kg^{-1}] ^[h]	3231	459	2278	1291
$\Delta H_{\text{f}}^\circ$ [kJ kg^{-1}] ^[i]	3100	336	2180	1175

[a] Chemical melting point (DSC onsets) from measurement with $\beta = 2^\circ\text{C min}^{-1}$. [b] Decomposition point (DSC onsets) from measurement with $\beta = 2^\circ\text{C min}^{-1}$. [c] Nitrogen percentage. [d] Combined nitrogen and oxygen percentages. [e] Oxygen balance according to reference [66]. [f] Density from X-ray measurements. [g] Calculated constant pressure heat of combustion. [h] Standard heat of formation (back-calculated from ΔH_{comb}). [i] Standard heat of formation.

Table 5. Physicochemical properties of methylguanazinium salts **6**, **6a**, **7** and **7a**.

	6	6a	7	7a
formula	$\text{C}_8\text{H}_{20}\text{N}_{22}\text{O}$	$\text{C}_8\text{H}_{18}\text{N}_{22}$	$\text{C}_4\text{H}_{11}\text{N}_{11}\text{O}_3$	$\text{C}_4\text{H}_9\text{N}_{11}\text{O}_2$
M_r [g mol^{-1}]	440.46	422.38	261.24	243.19
T_{m} [$^\circ\text{C}$] ^[a]	–	–	162	–
T_{d} [$^\circ\text{C}$] ^[b]	201	–	196	–
N [%] ^[c]	70.0	73.0	59.0	63.4
$N + O$ [%] ^[d]	73.6	73.0	77.4	76.5
Ω [%] ^[e]	-90.8	-94.7	-64.3	-69.1
ρ [g cm^{-3}] ^[f]	1.575	≈ 1.575	1.584	≈ 1.584
ΔH_{comb} [cal g^{-1}] ^[g]	–	-4251	–	-3321
$\Delta U_{\text{c}}^\circ$ [kJ kg^{-1}] ^[h]	4182	4361	2091	2246
$\Delta H_{\text{f}}^\circ$ [kJ kg^{-1}] ^[i]	4070	4244	1986	2134

[a] Chemical melting point (DSC onsets) from measurement with $\beta = 2^\circ\text{C min}^{-1}$. [b] Decomposition point (DSC onsets) from measurement with $\beta = 2^\circ\text{C min}^{-1}$. [c] Nitrogen percentage. [d] Combined nitrogen and oxygen percentages. [e] Oxygen balance according to reference [66]. [f] Density from X-ray measurements. [g] Calculated constant pressure heat of combustion. [h] Standard heat of formation (back-calculated from ΔH_{comb}). [i] Standard heat of formation.

Table 6. Initial safety testing results and predicted (calculated) energetic performance of methylguanazinium salts **3–8**, **6a** and **7a** using the EXPLO5 code.

	T_{ex} [K] ^[a]	V_0 [L kg^{-1}] ^[b]	P [GPa] ^[c]	D [m s^{-1}] ^[d]	Impact [J] ^[e]	Friction [N] ^[f]	Thermal shock
3	5829	762	27.5	8719	> 40	320	deflagrates
4	3030	843	25.8	8270	> 40	> 360	burns
5	–	–	–	–	25	220	deflagrates
6	3362	816	28.6	8922	> 40	> 360	deflagrates
6a	3242	797	27.7	8834	–	–	–
7	3442	829	25.6	8330	> 40	> 360	burns
7a	3233	797	23.9	8117	–	–	–
8	3736	837	27.7	8383	20	360	deflagrates
TNT	3736	620	20.5	7171	15	355	explodes
RDX	4334	796	34.0	8885	7.4	120	explodes

[a] Temperature of the explosion gases. [b] Volume of the explosion gases. [c] Detonation pressure. [d] Detonation velocity. [e] Tests according to BAM methods (see references [63–65]).

impact than TNT (15 J) and RDX (7.4 J), less sensitive to friction than RDX (120 N) and, except for compounds **3** (320 N) and **5** (220 N), they are also less sensitive to friction than TNT (355 N).^[70]

Tables 4 and 5 also contain the physicochemical properties of salts **3–8** (including **6a** and **7a**). The densities range from low ($\rho_{\text{calcd}}(\mathbf{3})=1.399 \text{ g cm}^{-3}$) to moderate ($\rho_{\text{calcd}}(\mathbf{5})=1.669 \text{ g cm}^{-3}$) and the predicted constant pressure heats of combustion (ΔH_{comb}), calculated by the MP2 method, are -4186 (**3**), -3165 (**4**), -2873 (**5**), -4251 (**6a**), -3321 (**7a**) and -2788 cal g^{-1} (**8**). The heats of formation are all positive and tend to decrease with decreasing nitrogen content apart from azotetrazolate salts **6** and **6a**, which have outstandingly high values (4100 kJ kg^{-1}), and the perchlorate salt (**5**), which regardless of the lowest nitrogen content has a very positive heat of formation (2180 kJ kg^{-1}). From the experimentally determined densities (X-ray), chemical compositions and energies of formation (back-calculated from the predicted heats of combustion) the detonation pressures and velocities of **3** (8719 ms^{-1} , 27.5 GPa), **4** (8270 ms^{-1} , 25.8 GPa), **6** (8922 ms^{-1} , 28.6 GPa), **6a** (8834 ms^{-1} , 27.7 GPa), **7** (8330 ms^{-1} , 25.6 GPa), **7a** (8117 ms^{-1} , 23.9 GPa) and **8** (8383 ms^{-1} , 27.7 GPa) were predicted using the EXPLO5 code.^[71] The following values for the empirical constants in the Becker–Kistiakowsky–Wilson equation of state (BKWN-EOS): $\alpha=0.5$, $\beta=0.176$, $\kappa=14.71$ and $\theta=6620$, were used. Due to the non-availability of a suitable method for the calculation of detonation parameters of compounds containing atoms others than C, H, N and O, compound **5** was excluded of this section. At this point it is important to point out that the predicted performances based on theoretical heats of combustion calculated by the above-mentioned method, tend to overestimate the values. In any case, taking into account this systematic overestimation, all compounds are predicted to outperform TNT (7171 ms^{-1} , 20.5 GPa) and salts **3**, **6** and **6a** have predicted values comparable to RDX (8885 ms^{-1} , 34.0 GPa).

Due to the negative oxygen balance of the salts studied here (-42 to -98%), it is of interest to analyse the performance of mixtures of the compounds **3**, **4** and **6–8** (including **6a** and **7a**) with an oxidiser such as ammonium nitrate (AN) or ammonium dinitramide (ADN) at an approximately oxygen neutral ratio ($\Omega \approx 0\%$) in order to further enhance their performances. The results of the EXPLO5 calculations are summarised in the Tables S9–S12 in the Supporting Information. Formulations of the compounds with AN show, in general, no increase in the performance (a more substantial decrease for compounds **3**, **6** and **6a**) and highly negative energies of formation ($\approx -3000 \text{ kJ kg}^{-1}$). On the other side, mixtures with ADN are predicted to have less negative heats of formation (positive values for the azotetrazolate salts **6** and **6a**) and better performances in all cases in comparison to the stand-alone energetic materials. The latter have high values between 31.3 and 33.7 GPa for the detonation pressures and between 8801 and 9077 ms^{-1} for the detonation velocities, which are similar to the predicted performance of mixtures of RDX and ADN.^[57b]

Conclusion

A new family of energetic salts based on the novel nitrogen-rich methylguanazinium cation have been synthesised in high yields and bulk purities and were characterised fully, including X-ray structure analysis. The hydrogen-bonding networks observed in the crystal structures were assessed by means of graph-set analysis. The nitrate and perchlorate anions seem to increase the decomposition points of the compounds, whereas the 5-nitrotetrazolate (**7**) and dinitramide (**8**) salts have lower thermal stabilities. Aside from **8**, all materials exhibit excellent thermal stabilities ($>190^\circ\text{C}$). All compounds have moderate densities $>1.4 \text{ g cm}^{-3}$, which are, in general, in the range of currently used explosives ($1.6\text{--}1.8 \text{ g cm}^{-3}$) and excellent combined oxygen and nitrogen balances, which are interesting from an environmental point of view. Additionally, all materials can be classified as insensitive or having a low sensitivity to classical stimuli. Formulations with AN are predicted to decrease the detonation parameters, whereas ADN increases them substantially. Lastly, the predicted detonation parameters of all compounds are higher than those of conventionally used TNT and those of the azide (**3**) and 5,5'-azotetrazolate (**6** and **6a**) salts indicate comparable performances to RDX, which suggest their potential as high explosives.

Experimental Section

Caution! Silver azide, silver dinitramide and their derivatives are energetic materials that tend to explode under certain conditions. Although we had no difficulties during the preparation and handling of the compounds described below, they are nevertheless energetic materials and their synthesis should be carried out by experienced personnel. In any case, proper protective measures such as Kevlar gloves, ear protection, safety shoes and plastic spatulas, should be taken at all times especially when working on a large scale ($>1 \text{ g}$).

General: All chemical reagents and solvents of analytical grade were obtained from Sigma–Aldrich and used as supplied. Methylguanazinium iodide,^[26] silver dinitramide, silver(bispyridine) dinitramide,^[27] sodium azotetrazolate pentahydrate^[28] and silver 5-nitrotetrazolate^[29] were prepared according to literature procedures. ^1H , ^{13}C , and $^{14}\text{N}/^{15}\text{N}$ NMR spectra were recorded on a JEOL Eclipse 400 instrument. The spectra were measured in $[\text{D}_6]\text{DMSO}$ at 25°C . The chemical shifts are given relative to tetramethylsilane (^1H , ^{13}C) or nitromethane ($^{14}\text{N}/^{15}\text{N}$) as external standards. Coupling constants (J) are given in hertz (Hz). Infrared (IR) spectra were recorded on a Perkin–Elmer Spectrum One FT-IR instrument as KBr pellets at room temperature. Raman spectra were recorded on a Perkin–Elmer Spectrum 2000R NIR FT-Raman instrument equipped with a Nd:YAG laser (1064 nm). The intensities are reported in percentages relative to the most intense peak and are given in parentheses. Elemental analyses were performed with a Netsch Simultaneous Thermal Analyzer STA 429. Melting points were determined by differential scanning calorimetry (Linseis DSC PT-10 instrument, calibrated with standard pure indium and zinc). Measurements were performed at a heating rate of $\beta=2^\circ\text{C min}^{-1}$ in closed aluminium containers with a hole (1 mm) on the top for gas release with a nitrogen flow of 20 mL min^{-1} . The reference sample was a closed aluminium container.

Synthesis of methylguanazinium azide (3): Freshly prepared silver azide (0.367 g , 2.45 mmol) was suspended in methanol (10 mL) and **2** (0.424 g , 2.04 mmol) was added with immediate precipitation of yellow silver iodide. The suspension containing an excess of silver azide was filtered

after 90 min reaction time into diethyl ether (80 mL) causing precipitation of a slightly pink product, which was filtered under gravity, washed with diethyl ether and recrystallised from diethyl ether/methanol yielding single crystals of the compound (0.181 g, 72%). DSC (2°C min⁻¹): 212 (m.p.), ≈215°C (decomp); ¹H NMR ([D₆]DMSO, 400.18 MHz, 25°C, TMS): δ = 8.06 (s, 2H; N₄H₂), 6.49 (s, 2H; N₆H₂), 5.68 (s, 2H; N₅H₂), 3.43 ppm (s, 3H; CH₃); ¹³C{¹H} NMR ([D₆]DMSO, 100.63 MHz, 25°C, TMS): δ = 150.5 (1C; C-N₅H₂), 147.6 (1C; C-N₆H₂), 34.2 ppm (1C; CH₃); ¹⁴N{¹H} NMR ([D₆]DMSO, 40.55 MHz, 25°C, MeNO₂): δ = -132.8 (N₁N), -276.9 ppm (N₁N); ¹⁵N NMR ([D₆]DMSO, 40.55 MHz, 25°C, MeNO₂): δ = -134.2 (N₁N), -164.8 (1N; N₃), -239.0 (1N; N₁), -240.5 (1N; N₂), -277.9 (N₁N), -321.9 (t, *J* = 74.9 Hz, 1N; N₄H₂), -322.4 (t, *J* = 80.5 Hz, 1N; N₅H₂), -335.4 ppm (t, *J* = 85.2 Hz, 1N; N₆H₂); Raman: $\tilde{\nu}$ (rel. int.) = 3174 (6), 2942 (7), 2812 (4), 1713 (21), 1667 (15), 1464 (13), 1417 (13), 1373 (5), 1347 (83), 1246 (14), 1200 (13), 1116 (12), 890 (8), 775 (56), 650 (32), 618 (11), 590 (12), 357 (18), 321 (31), 273 (11), 174 cm⁻¹ (29); IR (KBr): $\tilde{\nu}$ = 3324 (s), 3263 (s), 3192 (s), 3086 (s), 2039 (s), 1699 (s), 1660 (s), 1604 (m), 1574 (m), 1536 (w), 1462 (m), 1423 (w), 1384 (w), 1331 (w), 1242 (w), 1099 (m), 1022 (w), 881 (w), 777 (w), 712 (w), 649 (m), 587 (w), 486 (w), 348 cm⁻¹ (w); MS (FAB⁺, xenon, 6 keV, *m*-NBA matrix): *m/z*: 129.3 (cation); elemental analysis calcd (%) for C₃H₉N₉: C 21.05, H 5.30, N 73.65; found: C 21.10, H 5.31, N 73.41.

Synthesis of methylguanazinium nitrate (4): Compound **2** (1.700 g, 6.64 mmol) was treated, at room temperature with silver nitrate (1.180 g, 6.95 mmol) in water (30 mL) and the reaction mixture was stirred for 30 min. Silver iodide immediately precipitated as a brownish solid, which was filtered and the filtrate was concentrated in vacuo at 60°C giving pale pink single crystals of **4** upon cooling (0.931 g, 73%). DSC (2°C min⁻¹): 258 (m.p.), ≈261°C (decomp); ¹H NMR ([D₆]DMSO, 400.18 MHz, 25°C, TMS): δ = 7.94 (s, 2H; N₄H₂), 6.45 (s, 2H; N₆H₂), 5.69 (s, 2H; N₅H₂), 3.41 ppm (s, 3H; CH₃); ¹³C{¹H} NMR ([D₆]DMSO, 100.63 MHz, 25°C, TMS): δ = 150.5 (1C; C-N₅H₂), 147.6 (1C; C-N₆H₂), 34.2 ppm (1C; CH₃); ¹⁴N{¹H} NMR ([D₆]DMSO, 40.55 MHz, 25°C, MeNO₂): δ = -4.1 ppm (1N; NO₃); ¹⁵N NMR ([D₆]DMSO, 40.55 MHz, 25°C, MeNO₂): δ = -4.6 (NO₃), -164.6 (1N; N₃), -238.8 (1N; N₁), -240.3 (1N; N₂), -322.8 (t, *J* = 75.8 Hz, 1N; N₄H₂), -323.7 (t, *J* = 90.8 Hz, 1N; N₅H₂), -336.0 ppm (t, *J* = 87.5 Hz, 1N; N₆H₂); Raman: $\tilde{\nu}$ (rel. int.) = 3214 (8), 2953 (8), 2402 (15), 1703 (20), 1652 (2), 1471 (23), 1425 (20), 1393 (26), 1049 (100), 916 (11), 775 (18), 716 (19), 627 (25), 589 (15), 304 cm⁻¹ (18); IR (KBr): $\tilde{\nu}$ = 3349 (s), 3278 (s), 3150 (s), 2948 (m), 2424 (w), 1704 (s), 1656 (s), 1578 (m), 1538 (m), 1465 (m), 1423 (m), 1383 (s), 1327 (s), 1301 (s), 1209 (m), 1082 (m), 1046 (m), 1024 (m), 885 (m), 828 (m), 775 (m), 719 (m), 678 (w), 586 (m), 548 (m), 418 (m), 350 (m), 303 (w), 289 (w), 279 cm⁻¹ (w); MS (FAB⁺, xenon, 6 keV, *m*-NBA matrix): *m/z*: 129.3 (cation); elemental analysis calcd (%) for C₃H₉N₇O₃: C 18.85, H 4.75, N 51.29; found: C 18.73, H 4.85, N 51.25.

Synthesis of methylguanazinium perchlorate (5): Anhydrous silver perchlorate was weighed out in a glove box (0.754 g, 3.64 mmol) and dissolved into water (10 mL). Neat **2** (0.931 g, 3.64 mmol) was added portionwise with immediate precipitation of yellow silver iodide. The reaction mixture was stirred at room temperature and under exclusion of light for 1.5 h, after which time the solution was filtered into a glass shell and left to evaporate overnight yielding pure crystalline **5** (0.831 g, quant. yield). The crystals could be used for diffraction measurements. DSC (2°C min⁻¹): 247 (m.p.), ≈310°C (decomp); ¹H NMR ([D₆]DMSO, 400.18 MHz, 25°C, TMS): δ = 7.92 (s, 2H; N₄H₂), 6.47 (s, 2H; N₆H₂), 5.61 (s, 2H; N₅H₂), 3.41 ppm (s, 3H; CH₃); ¹³C{¹H} NMR ([D₆]DMSO, 100.63 MHz, 25°C, TMS): δ = 150.5 (1C; C-N₅H₂), 147.5 (1C; C-N₆H₂), 34.2 ppm (1C; CH₃); ¹⁵N NMR ([D₆]DMSO, 40.55 MHz, 25°C, MeNO₂): δ = -164.7 (1N; N₃), -238.7 (1N; N₁), -240.6 (1N; N₂), -323.1 (t, *J* = 75.8 Hz, 1N; N₄H₂), -324.0 (t, *J* = 91.2 Hz, 1N; N₅H₂), -336.2 ppm (t, *J* = 88.1 Hz, 1N; N₆H₂); ³⁵Cl NMR ([D₆]DMSO, 39.21 MHz, 25°C, NaCl): δ = 1.0 ppm (ClO₄); Raman: $\tilde{\nu}$ (rel. int.) = 3303 (4), 2994 (3), 2949 (7), 2818 (2), 1710 (27), 1649 (11), 1580 (10), 1476 (9), 1426 (14), 1334 (13), 1248 (8), 1134 (10), 936 (100), 777 (48), 651 (34), 629 (18), 588 (12), 462 (29), 332 (13), 306 cm⁻¹ (16); IR (KBr): $\tilde{\nu}$ = 3382 (s), 3327 (s), 3258 (s), 3085 (s), 1699 (s), 1658 (vs), 1461 (w), 1424 (w), 1384 (m), 1332 (w), 1260 (w), 1144 (s), 1113 (s), 1087 (vs), 907 (w), 778 (w), 712 (w), 636 (w), 626 (m), 587 (w), 476 (w), 350 (w), 321 (w), 302 cm⁻¹ (w); MS (FAB⁺,

xenon, 6 keV, *m*-NBA matrix): *m/z*: 129.1 (cation); elemental analysis calcd (%) for C₃H₉N₆O₄Cl: C 15.76, H 3.97, N 36.76, Cl 15.51; found: C 15.76, H 3.96, N 36.48, Cl 15.40.

Bis(methylguanazinium) 5,5'-azotetrazolate monohydrate (6): Compound **2** (1.025 g, 4.00 mmol) was heated to reflux with sodium azotetrazolate pentahydrate (0.600 g, 2.00 mmol) in water (20 mL) for 45 min. The reaction mixture was left to cool giving a first crop (0.569 g) of **6**. The volume of the orange filtrate was reduced and cooled in a refrigerator yielding slightly orange single crystals of the same product (0.168 g). The total amount of **6** obtained was 0.737 g (84%). DSC (2°C min⁻¹): ≈90 (H₂O loss), ≈198°C (decomp); ¹H NMR ([D₆]DMSO, 400.18 MHz, 25°C, TMS): δ = 8.14 (s, 2H; N₄H₂), 6.55 (s, 2H; N₆H₂), 5.79 (s, 2H; N₅H₂), 3.43 ppm (s, 3H; CH₃); ¹³C{¹H} NMR ([D₆]DMSO, 100.63 MHz, 25°C, TMS): δ = 173.1 (2C; C-N=N), 150.4 (1C; C-N₅H₂), 147.6 (1C; C-N₆H₂), 34.2 ppm (1C; CH₃); ¹⁵N NMR ([D₆]DMSO, 40.55 MHz, 25°C, MeNO₂): δ = 107.5 (-N=N-), 12.4 (CN_o), -66.5 (CN_i), -164.6 (1N; N₃), -239.1 (1N; N₁), -240.4 (1N; N₂), -322.7 (t, *J* = 79.1 Hz, 1N; N₄H₂), -323.2 (t, *J* = 88.9 Hz, 1N; N₅H₂), -335.4 ppm (t, *J* = 87.6 Hz, 1N; N₆H₂); Raman: $\tilde{\nu}$ (rel. int.) = 3188 (6), 1710 (2), 1615 (2), 1488 (60), 1410 (20), 1373 (100), 1348 (3), 1160 (2), 1088 (6), 1084 (18), 1072 (11), 1058 (23), 919 (9), 780 (5), 647 (2), 594 (2), 333 cm⁻¹ (2); IR (KBr): $\tilde{\nu}$ = 3328 (s), 3256 (s), 3047 (s), 2803 (m), 1708 (s), 1663 (s), 1620 (m), 1592 (m), 1532 (w), 1456 (w), 1385 (m), 1242 (w), 1192 (w), 1157 (w), 1118 (w), 1049 (w), 1029 (w), 957 (w), 897 (w), 872 (w), 774 (m), 726 (w), 643 (m), 587 (w), 558 (w), 452 (w), 360 (w), 332 (w), 320 (w), 296 (w), 285 (w), 205 cm⁻¹ (w); MS (FAB⁺, xenon, 6 keV, *m*-NBA matrix): *m/z*: 129.3 (cation); MS (FAB⁻, xenon, 6 keV, *m*-NBA matrix): *m/z*: 164.1 (anion); elemental analysis calcd (%) for C₈H₂₀N₂₂O: C 21.82, H 4.58, N 69.97; found: C 21.67, H 4.74, N 69.88.

Synthesis of methylguanazinium 5-nitrotetrazolate monohydrate (7): Sodium 5-nitrotetrazolate dihydrate (0.286 g, 1.91 mmol) was dissolved in water (3 mL) and a solution of silver nitrate (0.481 g, 2.99 mmol) in water (5 mL) was added dropwise with immediate precipitation of highly explosive white silver 5-nitrotetrazolate. The suspension was stirred for a couple of minutes and centrifuged. The liquid was decanted and the solid washed one time with water (5 mL) and one time with methanol (5 mL) with subsequent centrifuging. The liquid was decanted in both cases and the silver salt was suspended in methanol (10 mL) before neat **2** (0.417 g, 1.628 mmol) was added portionwise. Silver iodide immediately precipitated and the reaction mixture was stirred for 1.5 h, after which time the insoluble solid was filtered and the methanol evaporated to dryness giving the crude product, which could be recrystallised by diethyl ether diffusion into a saturated methanol solution of **7**, yielding pure crystalline material, which could be used to measure the crystal structure (0.308 g, 73%). DSC (2°C min⁻¹): ≈85 (H₂O loss), 162 (m.p.), ≈196°C (decomp); ¹H NMR ([D₆]DMSO, 400.18 MHz, 25°C, TMS): δ = 7.92 (s, 2H; N₄H₂), 6.42 (s, 2H; N₆H₂), 5.62 (s, 2H; N₅H₂), 3.68 (s, 2H; H₂O), 3.37 ppm (s, 3H; CH₃); ¹³C{¹H} NMR ([D₆]DMSO, 100.63 MHz, 25°C, TMS): δ = 168.9 (1C; C-NO₂), 150.8 (1C; C-N₅H₂), 147.9 (1C; C-N₆H₂), 34.6 ppm (1C; CH₃); ¹⁵N NMR ([D₆]DMSO, 40.55 MHz, 25°C, MeNO₂): δ = 18.7 (2N; N₉/10), -22.9 (1N; NO₂), -62.5 (2N; N₈/11), -164.0 (1N; N₃), -238.3 (1N; N₁), -239.9 (1N; N₂), -321.1 (t, *J* = 79.98 Hz, 1N; N₄H₂), -322.2 (t, *J* = 75.70 Hz, 1N; N₅H₂), -335.4 (t, *J* = 87.70 Hz, 1N; N₆H₂); Raman: $\tilde{\nu}$ (rel. int.) = 3138 (3), 2959 (4), 1712 (10), 1662 (10), 1546 (15), 1447 (14), 1418 (100), 1320 (11), 1184 (9), 1162 (10), 1068 (57), 1051 (31), 900 (6), 836 (13), 782 (26), 647 (13), 623 (7), 591 (7), 538 (6), 321 (10), 260 (7), 239 cm⁻¹ (8); IR (KBr): $\tilde{\nu}$ = 3379 (s), 3327 (s), 3255 (s), 3089 (s), 2730 (w), 2464 (w), 2092 (w), 1700 (s), 1657 (s), 1545 (s), 1444 (s), 1419 (s), 1384 (m), 1343 (w), 1317 (m), 1241 (w), 1173 (w), 1161 (w), 1101 (m), 1060 (w), 1050 (w), 1031 (w), 963 (w), 903 (w), 839 (w), 832 (w), 780 (w), 712 (w), 625 (w), 588 (w), 472 cm⁻¹ (w); *m/z* (FAB⁺, xenon, 6 keV, *m*-NBA matrix): 129.1 (cation); MS (FAB⁻, xenon, 6 keV, *m*-NBA matrix): 114.0 (anion); C₄H₁₁N₁₁O₃: C 18.39, H 4.24, N 58.99; found: C 18.29, H 4.28, N 58.82.

Synthesis of methylguanazinium dinitramide (8)

Method 1: A fresh hot solution of silver dinitramide (0.446 g, 3.04 mmol) in methanol (50 mL) was added into a solution of **2** (0.632 g, 3.04 mmol) in methanol (5 mL) at room temperature. Immediate precipitation of

yellow silver iodide was observed and the reaction mixture was stirred for further 45 min under exclusion of light. The crude product was precipitated by addition of diethyl ether (300 mL) and recrystallised by diethyl ether diffusion into a concentrated methanolic solution. The overall yield over two steps is 42% (0.301 g).

Method 2: Alternatively, **8** was synthesised in a safer way as follows. Silver dinitramide bispyridine (0.277 g, 1.05 mmol) was dissolved in methanol (5 mL) and neat methylguanazinium iodide (0.218 g, 1.05 mmol) was added causing precipitation of yellow silver iodide. The suspension was stirred for 1 h under exclusion of light and the yellow residue was filtered. Diethyl ether (60 mL) was added to the filtrate causing precipitation of a white solid, which was filtered under vacuum. The crude product could be purified by allowing diethyl ether to slowly diffuse into a saturated solution of **8** overnight yielding single crystals of the compound (0.147 g, 75%). DSC (2°C min⁻¹): 129 (m.p.), ≈160°C (decomp); ¹H NMR ([D₆]DMSO, 400.18 MHz, 25°C, TMS): δ = 7.93 (s, 2H; N4H₂), 6.47 (s, 2H; N6H₂), 5.62 (s, 2H; N5H₂), 3.41 ppm (s, 3H; CH₃); ¹³C{¹H} NMR ([D₆]DMSO, 100.63 MHz, 25°C, TMS): δ = 150.5 (1C; C-N5H₂), 147.5 (1C; C-N6H₂), 34.2 ppm (1C; CH₃); ¹⁴N{¹H} NMR ([D₆]DMSO, 40.55 MHz, 25°C, MeNO₂): δ = -10.1 ppm (2N; N(NO₂)₂); ¹⁵N NMR ([D₆]DMSO, 40.55 MHz, 25°C, MeNO₂): δ = -11.1 (N(NO₂)₂), -164.5 (1N; N3), -177.8 (N(NO₂)₂), -238.8 (1N; N1), -240.5 (1N; N2), -322.5 (t, J = 76.5 Hz, 1N; N4H₂), -323.5 (t, J = 91.9 Hz, 1N; N5H₂), -335.9 ppm (t, J = 84.8 Hz, 1N; N6H₂); Raman ν(rel. int.) = 3200 (6), 2954 (7), 1706 (20), 1649 (10), 1577 (9), 1473 (10), 1437 (18), 1421 (15), 1312 (100), 1220 (10), 1090 (3), 1174 (10), 1118 (10), 1047 (11), 1014 (9), 959 (12), 911 (7), 823 (37), 777 (48), 649 (31), 588 (11), 545 (7), 488 (21), 452 (8), 338 (20), 300 (37), 192 cm⁻¹ (13); IR (KBr): $\tilde{\nu}$ = 3381 (m), 3327 (m), 3258 (s), 3086 (s), 1699 (m), 1658 (vs), 1613 (w), 1537 (m), 1431 (m), 1384 (w), 1343 (w), 1205 (s), 1178 (s), 1097 (w), 1032 (m), 953 (vw), 905 (vw), 828 (vw), 778 (w), 761 (w), 732 (w), 712 (w), 648 (w), 587 (w), 470 cm⁻¹ (w); MS: (FAB⁺, xenon, 6 keV, m-NBA matrix): 129.3 (cation); elemental analysis calcd (%) for C₃H₉N₉O₄: C 15.32, H 3.86, N 53.61; found: C 15.21, H 3.77, N 53.88.

Acknowledgements

Financial support of this work by the Ludwig-Maximilian University of Munich (LMU), the Fonds der Chemischen Industrie (FCI), the European Research Office (ERO) of the U.S. Army Research Laboratory (ARL) and ARDEC (Armament Research, Development and Engineering Center) under contract nos. N 62558-05-C-0027, R&D 1284-CH-01, R&D 1285-CH-01, 9939-AN-01 and W911NF-07-1-0569 and the Bundeswehr Research Institute for Materials, Explosives, Fuels and Lubricants (WIWEB) under contract nos. E/E210/4D004/X5143 and E/E210/7D002/4F088 is gratefully acknowledged. The authors acknowledge collaborations Dr. M. Krupka (OZM Research, Czech Republic) in the development of new testing and evaluation methods for energetic materials and with Dr. M. Sucasca (Brodarski Institute, Croatia) in the development of new computational codes to predict the detonation parameters of high-nitrogen explosives. We are indebted to and thank Dr. Betsy M. Rice (ARL, Aberdeen, Proving Ground) for many helpful and inspired discussions and support of our work.

- [1] a) T. M. Klapötke, C. M. Rienäcker, H. Zewen, *Z. Anorg. Allg. Chem.* **2002**, *628*, 2372–2374; b) H.-G. Ang, W. Fraenk, K. Karaghiosoff, T. M. Klapötke, P. Mayer, H. Nöth, J. Sprott, M. Warchhold, *Z. Anorg. Allg. Chem.* **2002**, *628*, 2894–2900.
- [2] K. Karaghiosoff, T. M. Klapötke, A. Michailovski, G. Holl, *Acta Crystallogr. Sect. C* **2002**, *58*, 580–581.
- [3] a) J. Geith, T. M. Klapötke, J. J. Weigand, G. Holl, *Propellants Explos. Pyrotech.* **2004**, *29*, 3–8; b) M. von Denffer, T. M. Klapötke, G. Kramer, G. Spiess, J. M. Welch, G. Heeb, *Propellants Explos. Pyrotech.* **2005**, *30*, 191–195; c) T. M. Klapötke, K. Karaghiosoff, P. Mayer, A. Penger, J. M. Welch, *Propellants Explos. Pyrotech.* **2006**, *31*, 188–195; d) R. Böse, T. M. Klapötke, P. Mayer, V. Verma, *Propellants Explos. Pyrotech.* **2006**, *31*, 263–268.
- [4] A. Hammerl, M. A. Hiskey, G. Holl, T. M. Klapötke, K. Polborn, J. Stierstorfer, J. J. Weigand, *Chem. Mater.* **2005**, *17*, 3784–3793.
- [5] G. Majano, S. Mintova, T. Bein, T. M. Klapötke, *Adv. Mater.* **2006**, *18*, 2240–2243.
- [6] J. Evers, T. M. Klapötke, P. Mayer, G. Oehlinger, J. M. Welch, *Inorg. Chem.* **2006**, *45*, 4996–5007.
- [7] a) M. Göbel, T. M. Klapötke, P. C. Thumbs, *Proceed. 9th Sem. New Trends Res. Energ. Mater.* (Pardubice, Czech Republic) **2006**, p. 127; b) T. M. Klapötke, P. Mayer, K. Polborn, J. M. Welch, *Proceed. 9th Sem. New Trends Res. Energ. Mater.* (Pardubice, Czech Republic) **2006**, p. 631; c) M. Göbel, K. Karaghiosoff, T. M. Klapötke, C. Miró Sabaté, *Chem. Mater.* **2008**, *20*, 1750–1763; Sabaté, *Z. Anorg. Allg. Chem.* **2007**, *633*, 2671–2677; J. M. Welch, *Proceed. 9th Sem. New Trends Res. Energ. Mater.* (Pardubice, Czech Republic) **2006**, p. 202.
- [8] T. M. Klapötke, *Nachr. Chem. Tech.* **2008**, *56*, 645–648.
- [9] Y. Huang, H. Gao, B. Twamley, J. M. Shreeve, *Eur. J. Inorg. Chem.* **2007**, *14*, 2025–2030.
- [10] H. Xue, H. Gao, B. Twamley, J. M. Shreeve, *Eur. J. Inorg. Chem.* **2006**, *15*, 2959–2965.
- [11] V. A. Ostrovskii, M. S. Pevzner, T. P. Kofman, M. B. Shcherbinin, I. V. Tselinskii, *Targets Heterocycl. Syst.* **1999**, *3*, 467–526.
- [12] a) D. E. Chavez, M. A. Hiskey, *J. Energ. Mater.* **1999**, *17*, 357–377; b) D. E. Chavez, M. A. Hiskey, D. L. Naud, *Propellants Explos. Pyrotech.* **2004**, *29*, 209–215.
- [13] a) A. Hammerl, G. Holl, M. Kaiser, T. M. Klapötke, P. Mayer, H. Nöth, H. Piotrowski, M. Warchhold, *Eur. J. Inorg. Chem.* **2002**, *4*, 834–845; b) A. Hammerl, G. Holl, T. M. Klapötke, P. Mayer, H. Nöth, H. Piotrowski, M. T. Suter, *Z. Naturforsch. B* **2001**, *56*, 857–870; c) J. Geith, T. M. Klapötke, J. J. Weigand, G. Holl, *Propellants Explos. Pyrotech.* **2004**, *29*, 3–8; d) T. M. Klapötke, P. Mayer, A. Shulz, J. J. Weigand, *Propellants Explos. Pyrotech.* **2004**, *29*, 325–332.
- [14] T. M. Klapötke, C. Miró Sabaté, *Z. Anorg. Allg. Chem.* **2007**, *633*, 2671–2677.
- [15] M. Göbel, K. Karaghiosoff, T. M. Klapötke, *Angew. Chem.* **2006**, *118*, 6183–6186; *Angew. Chem. Int. Ed.* **2006**, *45*, 6037–6040.
- [16] M. Göbel, T. M. Klapötke, *Z. Anorg. Allg. Chem.* **2007**, *633*, 1006–1017.
- [17] a) X.-J. Wang, S.-Y. Jia, B.-Z. Wang, P. Lian, C. Zhou, *Hanneng Cailiao* **2006**, *14*, 439–445; b) K. Y. Lee, C. B. Storm, M. A. Hiskey, M. D. Coburn, *J. Energ. Mater.* **1991**, *9*, 415–428.
- [18] a) H. G. O. Becker, V. Eisenschmidt, K. Wehner, DD 19670415, **1967**; b) W. P. Norris, R. A. Henry, *J. Org. Chem.* **1964**, *29*, 650–660.
- [19] H. Xue, Y. Gao, B. Twamley, J. M. Shreeve, *Chem. Mater.* **2005**, *17*, 191–198.
- [20] H. Xue, B. Twamley, J. M. Shreeve, *J. Mater. Chem.* **2005**, *15*, 3459–3465.
- [21] G. K. Williams, S. P. Burns, I. B. Mishra, WO 2005035466, **2005**.
- [22] A. R. Katritzky, S. Singh, K. Kirichenko, J. D. Holbrey, M. Smiglak, W. M. Reichert, R. D. Rogers, *Chem. Commun.* **2005**, *7*, 868–870.
- [23] a) R. G. Child, *J. Heterocycl. Chem.* **1965**, *2*, 98–99; b) C. Darwich, T. M. Klapötke, M. Sucasca, J. M. Welch, *Propellants Explos. Pyrotech.* **2007**, *32*, 235–243.
- [24] C. Darwich, Klapötke, C. Miró Sabaté, *Propellants, Explos. Pyrotech.* **2008**, in press.
- [25] a) G. W. Drake, T. W. Hawkins, L. A. Hall, J. A. Boatz, A. J. Brand, *Propellants Explos. Pyrotech.* **2005**, *30*, 329–337; b) G. W. Drake, US 6509473, **2003**.
- [26] C. Darwich, K. Karaghiosoff, T. M. Klapötke, C. Miró Sabaté, *Z. Anorg. Allg. Chem.* **2008**, *634*, 61–68.
- [27] H.-G. Ang, W. Fraenk, K. Karaghiosoff, T. M. Klapötke, P. Mayer, H. Nöth, J. Sprott, M. Warchhold, *Z. Anorg. Allg. Chem.* **2002**, *628*, 2894–2900.
- [28] a) J. Thiele, *Justus Liebigs Ann. Chem.* **1892**, *270*, 54–63; b) J. Thiele, J. T. Marais, *Justus Liebigs Ann. Chem.* **1893**, *273*, 144–160; c) J. Thiele, *Ber. Dtsch. Chem. Ges.* **1893**, *26*, 2645–2646; d) J. Thiele, *Justus Liebigs Ann. Chem.* **1898**, *303*, 57–75.

- [29] L. R. Bates, J. M. Jenkins, US 4094879, **1978**.
- [30] <http://www.cem.msu.edu/~reusch/VirtualText/acidity2.htm>.
- [31] J. C. Gálvez-Ruiz, G. Holl, K. Karaghiosoff, T. M. Klapötke, K. Löhnwitz, P. Mayer, H. Nöth, K. Polborn, C. J. Rohbogner, M. Suter, J. J. Weigand, *Inorg. Chem.* **2005**, *44*, 4237–4253.
- [32] U. Müller, *Struct. Bonding* **1974**, *14*, 141–145.
- [33] a) K. Williamson, P. Li, J. P. Devlin, *J. Chem. Phys.* **1968**, *48*, 3891–3896; b) J. R. Fernandes, S. Ganguly, C. N. R. Rao, *Spectrochim. Acta Part A* **1979**, *35*, 1013–1019.
- [34] a) H. Cohn, *J. Chem. Soc.* **1952**, 4282–4284; b) P. Redlich, J. Holt, T. Biegeleisen, *J. Am. Chem. Soc.* **1944**, *66*, 13–16; c) H. Grothe, H. Willner, *Angew. Chem.* **1996**, *108*, 816–818; *Angew. Chem. Int. Ed. Engl.* **1996**, *35*, 768–769.
- [35] K. O. Christe, W. W. Wilson, M. A. Petrie, H. H. Michels, J. C. Botaró, R. Gilardi, *Inorg. Chem.* **1996**, *35*, 5068–5071.
- [36] Gaussian 03, Revision A.1: M. J. Frisch, G. W. Trucks, H. B. Schlegel, G. E. Scuseria, M. A. Robb, J. R. Cheeseman, J. A. Montgomery, T. Jr Vreven, K. N. Kudin, J. C. Burant, J. M. Millam, S. S. Iyengar, J. Tomasi, V. Barone, B. Mennucci, M. Cossi, G. Scalmani, N. Rega, G. A. Petersson, H. Nakatsuji, M. Hada, M. Ehara, K. Toyota, R. Fukuda, J. Hasegawa, M. Ishida, T. Nakajima, Y. Honda, O. Kitao, H. Nakai, M. Klene, X. Li, J. E. Knox, H. P. Hratchian, J. B. Cross, C. Adamo, J. Jaramillo, R. Gomperts, R. E. Stratmann, O. Yazyev, A. J. Austin, R. Cammi, C. Pomelli, J. W. Ochterski, P. Y. Ayala, K. Morokuma, G. A. Voth, P. Salvador, J. J. Dannenberg, V. G. Zakrzewski, S. Dapprich, A. D. Daniels, M. C. Strain, O. Farkas, D. K. Malick, A. D. Rabuck, K. Raghavachari, J. B. Foresman, J. V. Ortiz, Q. Cui, A. G. Baboul, S. Clifford, J. Cioslowski, B. B. Stefanov, G. Liu, A. Liashenko, P. Piskorz, I. Komaromi, R. L. Martin, D. J. Fox, T. Keith, M. A. Al-Laham, C. Y. Peng, A. Nanayakkara, M. Challacombe, P. M. W. Gill, B. Johnson, W. Chen, M. W. Wong, C. Gonzalez, J. A. Pople, Gaussian, Inc. Pittsburgh PA, **2004**.
- [37] K. Karaghiosoff, T. M. Klapötke, P. Mayer, C. Miró Sabaté, A. Penger, J. M. Welch, *Inorg. Chem.* **2008**, *47*, 1007–1019.
- [38] H.-G. Ang, W. Fraenk, K. Karaghiosoff, T. M. Klapötke, H. Nöth, J. Sprott, M. Suter, M. Vogt, M. Warchhold, *Z. Anorg. Allg. Chem.* **2002**, *628*, 2901–2906.
- [39] A. Hammerl, T. M. Klapötke, H. Piotrowski, G. Holl, M. Kaiser, *Propellants Explos. Pyrotech.* **2001**, *26*, 161–164.
- [40] A. Hammerl, G. Holl, K. Hubler, M. Kaiser, T. M. Klapötke, P. Mayer, *Eur. J. Inorg. Chem.* **2001**, *3*, 755–760.
- [41] T. M. Klapötke, C. Miró Sabaté, *Proceed. 9th Sem. New Trends Res. Energ. Mater.* (Pardubice, Czech Republic) **2007**, p. 191.
- [42] A. Altomare, M. C. Burla, M. Camalli, G. L. Cascarano, C. Giacovazzo, A. Gagliardi, A. G. G. Moliterni, G. Polidori, R. Spagna, *J. Appl. Crystallogr.* **1999**, *32(1)*, 115–119.
- [43] M. Sheldrick, SHELXL-97, Program for Crystal Structure Refinement, Universität Göttingen, **1997**.
- [44] G. Drake, T. Hawkins, *Ionic Liquids Workshop*, Tampa, FL, March **2004**.
- [45] a) N. V. Podbereskaya, N. V. Pervukhina, V. P. Doronina, *Zh. Strukt. Khim.* **1991**, *32*, 34–39; b) C. Ye, J.-C. Xiao, B. Twamley, J. M. Shreeve, *Chem. Commun.* **2005**, *21*, 2750–2752.
- [46] a) C. Foces-Foces, F. H. Cano, R. M. Claramunt, D. Sanz, J. Catalan, F. Fabero, A. Fruchier, J. Elguero, *J. Chem. Soc. Perkin Trans. 2* **1990**, *2*, 237–244; b) R. M. Claramunt, D. Sanz, J. Catalan, F. Fabero, N. A. García, C. Foces-Foces, A. L. Llamas-Saiz, J. Elguero, *J. Chem. Soc. Perkin Trans. 2* **1993**, *9*, 1687–1699.
- [47] A. F. Hollemann, E. Wieberg, N. Wieberg in *Lehrbuch der Anorganischen Chemie*, 101th ed., Walter de Gruyter, Berlin, **1995**.
- [48] M. D. Harmony, V. W. Laurie, R. L. Kuczkowski, R. H. Schwedeman, D. A. Ramsay, F. L. Lovas, W. J. Lafferty, A. G. Maki, *J. Phys. Chem. Ref. Data* **1979**, *8*, 619–721.
- [49] J. Bernstein, R. E. Davis, L. Shimoni, N. L. Chang, *Angew. Chem.* **1995**, *107*, 1689–1708; *Angew. Chem. Int. Ed. Engl.* **1995**, *34*, 1555–1573.
- [50] RPLUTO, Cambridge Crystallographic Data Centre, Cambridge, UK, **2000**, <http://www.ccdc.cam.ac.uk/support/documentation/rpluto/TOC.html>.
- [51] *International Tables for X-ray Crystallography, Vol. C*, Kluwer Academic, Dordrecht, **1992**.
- [52] A. Bondi, *J. Phys. Chem.* **1964**, *68*, 441–451.
- [53] a) S. Asath Bahadur, R. K. Rajaram, M. Nethaki, *Acta Crystallogr. Sect. C* **1991**, *47*, 1420–1423; b) A. Wojtczak, M. Jaskólski, Z. Kosturkiewicz, *Acta Crystallogr. Sect. C* **1988**, *44*, 1779–1981.
- [54] a) M. Alfonso, Y. Wang, H. Stoeckli-Evans, *Acta Crystallogr. Sect. C* **2001**, *57*, 1184–1188; b) S.-C. Shao, D.-R. Zhu, X.-H. Zhu, X.-Z. You, R. S. Shanmuga H.-K. Fun, *Acta Crystallogr. Sect. C* **1999**, *55*, 1412–1413.
- [55] A. Hammerl, T. M. Klapötke, H. Nöth, M. Warchhold, H. Holl, M. Kaiser, *Inorg. Chem.* **2001**, *40*, 3570–3575.
- [56] M. A. Pierce-Butler, *Acta Crystallogr. Sect. B* **1982**, *38*, 2681–2683.
- [57] a) T. M. Klapötke, C. Miró Sabaté, *Proceed. ICT Symp. Insens. Energ. Mater.* (Pfinztal, Germany) **2007**; b) T. M. Klapötke, C. Miró Sabaté, *Chem. Mater.* **2008**, *20*, 1750–1763.
- [58] a) H. Xue, Y. Gao, B. Twamley, J. M. Shreeve, *Inorg. Chem.* **2005**, *44*, 5068–5072; b) T. M. Klapötke, K. Karaghiosoff, P. Mayer, A. Penger, J. M. Welch, *Propellants Explos. Pyrotech.* **2006**, *31*, 188–195; c) H. Xue, H. Gao, B. Twamley, J. M. Shreeve, *Chem. Mater.* **2007**, *19*, 1731–1739.
- [59] T. M. Klapötke, P. Mayer, C. Miró, A. Penger, J. M. Welch, *Abstr. Pap. 233rd ACS Nat. Meet.* (Chicago, USA) **2007**.
- [60] M. E. Sitzman, R. Gilardi, R. J. Butcher, W. M. Koppes, A. G. Stern, J. S. Trasher, N. J. Trivedi, Z.-Y. Yang, *Inorg. Chem.* **2000**, *39*, 843–850.
- [61] A. Martin, A. A. Pinkerton, R. D. Gilardi, J. C. Botarro, *Acta Crystallogr. Sect. B* **1997**, *53*, 504–512.
- [62] T. M. Klapötke, P. Mayer, A. Schulz, J. J. Weigand, *J. Am. Chem. Soc.* **2005**, *127*, 2032–2033.
- [63] T. M. Klapötke, C. M. Rienäcker, *Propellants Explos. Pyrotech.* **2001**, *26*, 43–47.
- [64] Tests methods according to the UN Recommendation on the Transport of Dangerous Goods, *Manual of Tests and Criteria*, 4th ed., United Nations Publications, New York, **2003**.
- [65] Reichel & Partner GmbH, <http://www.reichel-partner.de>.
- [66] Calculation of the oxygen balance: $\Omega(\%) = (\text{O} - 2\text{C} - \text{H}/2 - x\text{AO})/1600\text{M}$; M = molecular mass.
- [67] L. Glasser, H. D. B. Jenkins, D. Tudela, *Inorg. Chem.* **2002**, *41*, 2364–2367.
- [68] T. M. Klapötke, P. Mayer, C. Miró Sabaté, J. M. Welch, N. Wiegand, *Inorg. Chem.* **2008**, in press.
- [69] H. Gao, C. Ye, C. M. Piekarski, J. M. Shreeve, *J. Phys. Chem. C* **2007**, *111*, 10718–10731.
- [70] J. Koehler, R. Meyer in *Explosivstoffe*, 9th ed., Wiley-VCH, Weinheim, **1998**.
- [71] a) M. Sućeska, *Mater. Sci. For.* **2004**, 465; b) M. Sućeska, *Propellants Explos. Pyrotech.* **1991**, *16*, 197–202; c) M. Sućeska, *Propellants Explos. Pyrotech.* **1999**, *24*, 280–285.

Received: February 23, 2008
Published online: June 3, 2008